

# Testing the Disk Regulation Paradigm with Spitzer Observations.

## I.

### Rotation Periods of Pre-main Sequence Stars in the IC 348 Cluster

Lucas Cieza and Nairn Baliber

lcieza@astro.as.utexas.edu, baliber@astro.as.utexas.edu

*Astronomy Department, University of Texas at Austin  
University Station C1400, Austin, TX 78712*

#### ABSTRACT

We present 105 stellar rotation periods in the young cluster IC 348, 75 of which are new detections, increasing the total number of known periods in this cluster to 143. The period distribution resembles that seen in the heart of the Orion Nebula Cluster by Herbst and colleagues. Stars estimated to be less massive than  $0.25 M_{\odot}$  show a unimodal distribution of fast rotators ( $P \sim 1\text{--}2$  days) and a tail of slower rotators, while stars estimated to be more massive than  $0.25 M_{\odot}$  show a bimodal distribution with peaks at  $\sim 2$  and  $\sim 8$  days. We combine all published rotation periods in IC 348 with *Spitzer* mid-IR (3.6, 4.5, 5.8, and  $8.0 \mu\text{m}$ ) photometry, which provides an unprecedented efficient and reliable disk indicator in order to test the disk-braking paradigm. We find no evidence that the tail of slow rotators in low-mass stars or the long period peak in high-mass stars are preferentially populated by objects with disks as might be expected based on the current disk-braking model. Also, we find no significant correlation between period and the *magnitude* of the IR-excess, regardless of the mass range considered. Given the significant improvement of *Spitzer* observations over near-IR indicators of inner disks, our results *do not* support a strong correlation in this cluster between rotation period and the presence of a disk as predicted by disk-braking theory. Rather, they are consistent with the suggestion that the correlation between period and the amplitude of the (I–K) excess reported in the past is a secondary manifestation of the correlation between the amplitude of near-IR excess and mass. By comparing our sample with a recent *Spitzer* census of IC 348, we find

that the disk properties of our sample are indistinguishable from the overall disk properties of the cluster. We conclude that it is very unlikely that the lack of a correlation between rotation period and IR excess is due to a bias in the disk properties of our sample. Finally, we find some indication that the disk fraction decreases significantly for stars with very short periods ( $P \lesssim 1.5$  days). The fact that very fast rotators tend to have little or no excess has already been recognized by Rebull and colleagues for stars in the Orion Nebula Cluster. This is the only feature of our sample that could *potentially* be interpreted as evidence for disk braking. There is currently no alternative model to disk braking to explain the evolution of the angular momentum of pre-main-sequence stars. It has been proposed that the observational signatures of disk braking might be significantly masked by the intrinsic breadth of the initial period distribution. We argue that more rigorous modeling of angular momentum evolution and a quantitative analysis of the observational data are required before the disk-braking model can be regarded as inconsistent with observations.

*Subject headings:*

## 1. Introduction

The evolution of the angular momentum of pre-main-sequence (PMS) stars is one of the longest-standing problems in star formation and is currently a controversial topic. As low-mass ( $\sim 0.1\text{--}1.2 M_{\odot}$ ) PMS stars evolve along their convective tracks, conservation of angular momentum dictates that they should spin up considerably. Low-mass PMS stars are believed to contract by a factor of  $\sim 2\text{--}3$  during their first 3 Myrs of evolution. If these stars were to conserve their specific angular momentum,  $j$  (where  $j \propto R^2/P$ ), their rotation periods would be expected to decrease by a factor of  $\sim 4\text{--}9$ . Using the models by D’Antona & Mazzitelli (1994, 1998, D98, hereafter),<sup>1</sup> and assuming angular momentum conservation and homologous contraction, Herbst et al. (2000) show that, given a starting period of 10 days,<sup>2</sup> all low-mass stars should rotate with periods shorter than  $\sim 2$  days by an age of 2 Myrs. However, observations show a large population of slow rotators ( $P \sim 8.0$  days) in clusters that, according to the same evolutionary tracks, are  $\sim 2$  Myrs old or older (Luhman et al. 2003). Also, the *very* broad distribution of rotation periods in the zero-age main sequence

---

<sup>1</sup>Available at <http://www.mporzio.astro.it/dantona/prems.html>

<sup>2</sup>Adopting an initial period of 10 days is a conservative choice because recent observations (e.g. Covey et al. 2005) show that deeply embedded PMS stars tend to rotate *faster* than optically revealed PMS stars.

(ZAMS) suggests a very broad range of angular momentum loss between the birth line and the ZAMS.

Proposed mechanisms to explain the presence of slow rotators come in the form of magnetic-field interaction between the PMS star and material in its inner disk, locking the star’s rotation to the Keplerian velocity of the disk’s inner edge (Königl 1991; Shu et al. 1994) and/or creating an accretion-driven wind (Shu et al. 2000), thereby transferring angular momentum from the star to material from the disk, preventing it from spinning up, unchecked. “Disk locking” and “disk braking” have become essential features of virtually every model of the angular momentum evolution of PMS stars.

The first order prediction of disk-locking and disk-braking models is that, as a group, stars with disks should rotate slower than stars that have already lost their disks and are free to spin up. However, finding an observational correlation between the presence (or lack) of a circumstellar disk and the rotation period of PMS stars has proven a difficult task. It has been repeatedly argued that one of the main difficulties in finding this predicted correlation is the lack of an appropriate disk indicator (Rebull 2001; Herbst et al. 2002). *Spitzer*’s unprecedented mid-IR sensitivity allows, for the first time, an unambiguous identification of disks in a statistically significant sample of PMS stars with known rotation periods.

Here we report 75 previously unidentified rotation periods detected in the young cluster IC 348 which is situated in the East side of the Perseus Molecular Cloud. Our new periods, when combined with the periods in the literature, increase the total number of known periods in this cluster to 143. IC 348 is 315 pc away, young (2–3 Myrs), relatively compact ( $\sim 400$  members,  $D \sim 20$  arcminutes), and has low extinction ( $A_V < 4$ ) (Luhman et al. 2003). We combine all published rotation periods in IC 348 with *Spitzer* photometry to investigate the disk-braking scenario. This paper is organized as follows. In Section 2, we summarize previous observational attempts to identify a period–disk correlation. In Section 3, we describe our time series photometry and the observed rotation period distribution. In Section 4, we combine the rotation periods with the disk identification from *Spitzer* observations in order to search for the period–disk correlation predicted by the disk-braking paradigm. In section 5, we discuss the implication of our results in the context of the disk-braking scenario. Finally, we summarize our results in Section 6.

## 2. Previous Observational Results

### 2.1. Rotation Periods and Disks in Other Clusters

Rotation periods of young stars with late spectral types can efficiently be obtained via precise differential photometry due the brightness modulation produced by the rotation of cool star spots and hot accretion columns reaching their surfaces. Fifteen years ago, the number of PMS stars with photometrically measured rotation periods was less than 100. This number is currently approaching 2000 (see Stassun & Terndrup (2003) for a recent review of observations). As the number of available rotation periods of PMS stars in young stellar clusters has increased, some groups have found apparent observational signatures of the disk-locking model. Attridge & Herbst (1992) report a bimodal distribution in the period of 35 PMS stars in the Orion Nebula Cluster (ONC), peaking at  $\sim 2$  and  $\sim 8$  days. This bimodal distribution has been confirmed by Herbst et al. (2000, 2002, H00 and H02, hereafter), who find it to be restricted to samples of stars with masses  $> 0.25 M_{\odot}$ . H02 find that very low-mass stars ( $M < 0.25 M_{\odot}$ ) exhibit a unimodal period distribution dominated by fast rotators with periods of 1–2 days. H00 and H02 also report a positive correlation between the presence of a circumstellar disk (as indicated by the presence of K-band excess) and slow rotation. The long-period peak in the bimodal distribution has been interpreted by these authors as being populated by disk-locked stars.

However, observations by several other groups do not confirm the bimodal nature of the period distribution of PMS stars in the ONC. Based on a sample of 254 stars, Stassun et al. (1999) find that the distribution of rotation periods between 0.5 and 8.0 days is statistically consistent with a constant distribution and that there is no apparent correlation between rotation period and near-IR excess. H00 argue that the Stassun et al. (1999) results do not show the expected bimodal distribution because their sample is dominated by stars of very low mass (i.e.  $M < 0.25 M_{\odot}$ ). Still, based on 281 periods of stars in four fields *around* (but not including) the heart of the ONC, Rebull (2001) finds that the distribution of periods is statistically indistinguishable for stars less and more massive than  $0.25 M_{\odot}$ . Herbst & Mundt (2005) argue that the “Flanking Fields” observed by Rebull (2001) represent a very heterogeneous sample in terms of age in which any structure in the period distribution would be wiped out. Rebull (2001) also finds no clear correlation between the presence of a circumstellar disk and three different disk indicators ( $I_C-K$ ,  $H-K$ , and  $U-V$  color excesses). Rebull (2001) and Hillenbrand et al. (1998) show that the correlation between near-IR excess and disk presence is far from perfect, leading to many disks being missed and false identification of disks. Rebull (2001) does conclude, however, that, given the lack of any observable correlation, disk locking is probably not the complete solution to the period distribution of PMS stars.

More recently, a statistically significant number of rotation periods in NGC 2264 have become available. In this cluster, Lamm et al. (2005) find a bimodal distribution for a sample of 184 stars with estimated masses  $> 0.25 M_{\odot}$ . They find that the peaks in the period distribution observed in NGC 2264 are shifted toward shorter periods with respect to the ones found in the ONC. These shifts are interpreted as evidence of angular momentum evolution between the age of the ONC ( $\sim 1$  Myrs) and that of NGC 2264 ( $\sim 2\text{--}4$  Myrs). Using  $R\text{--}H\alpha$  color criteria for disk identification, they argue that stars with disks tend to rotate slower than stars without disks. However, 60% of their sample have ambiguous disk identification. Makidon et al. (2004) report periods for 118 stars in NGC 2264 with estimated masses  $> 0.25 M_{\odot}$ . They find no evidence for a statistically significant bimodal distribution or a disk–period correlation, regardless of the disk indicator used:  $EW(H\alpha)$ ,  $U\text{--}V$ ,  $I\text{--}K$ , or  $H\text{--}K$  color excesses. Clearly, despite the categorical claims made by some authors (e.g. Herbst & Mundt 2005), both the existence of a bimodal distribution in the rotation periods of PMS stars and the presence of a disk–rotation period correlation still await independent confirmation.

## 2.2. Rotation Periods and Disks in IC 348

All of the currently known periods for IC 348 can be collected from three papers (prior to this one): Cohen et al. (2004), Littlefair et al. (2005), and Kızıloğlu et al. (2005). Based on an observing campaign spanning more than 5 years, Cohen et al. (2004) report the rotation periods of 28 PMS stars in IC 348. The observations were taken in the  $I_C$  band with the 0.6 m telescope at the Van Vleck Observatory, which has a field of view of  $10'2$  on a side. Littlefair et al. (2005) report 32 additional periods based on  $I_C$  observations performed with the 1.0 m Jacobus Katelyn Telescope, which has a usable field of view of  $9'$  on a side. Cohen et al. (2004) and Littlefair et al. (2005) only report 18 periods in common (partially because the Littlefair et al. (2005) observations are considerably deeper than those presented by Cohen et al. (2004)), but the periods in common show excellent agreement. Finally, Kızıloğlu et al. (2005) present 35 periods based on observations taken with the 0.45 m ROTSE-IIIId robotic telescope which has a field of view of 1.85 degrees on a side and operates without a filter. Of these 35 periods, 17 were previously detected by Cohen et al. (2004), one was reported by Littlefair et al. (2005), and 18 were new detections. Kızıloğlu et al. (2005) calculated the confidence level of their rotation periods assuming white noise as the only source of error; however, as we discuss in Section 3.2, that is a very optimistic assumption. Therefore, we only use the rotation periods from their work which have confidence levels greater than  $5\sigma$ .

Cohen et al. (2004) do not have enough stars to fully explore the presence of a bimodal distribution or the disk–period correlation in their sample but argue that the period distribution hints at the bimodality seen in the ONC. Littlefair et al. (2005) also see a hint of a period bimodality in the “high” mass stars but argue that it is not statistically significant given the small number of stars in the appropriate mass range. They did explore the possibility of an observable disk–period correlation in their sample. However, they find no correlation of period with K–L color excess (available for 30 stars) or H $\alpha$  equivalent width (available for 43 stars). Also, Littlefair et al. (2005) suggest that the rotation period–(I–K) excess correlation reported by H02 might be due to a secondary correlation arising from the fact that (I–K) excess is easier to detect in stars more massive than  $0.25 M_{\odot}$  than it is to detect in lower-mass stars (Hillenbrand et al. 1998). The Kızılođlu et al. (2005) paper focuses on an X-ray luminosity–period correlation and does not discuss the shape of the period distribution or any possible correlation between period and disk indicators.

### 3. Optical Observations and Data Reduction

#### 3.1. Time Series Photometry

For our photometric measurements of IC 348 stellar rotation periods, data were collected using the McDonald Observatory 0.76 m Telescope and its Prime Focus Corrector (PFC) (Claver 1992), which provides a  $1^{\circ}$  field of view,  $46'2'' \times 46'2''$  of which is covered by a  $2048 \times 2048$  CCD. I<sub>C</sub>-band time-series photometry was performed on data collected during 3 observing runs: 2003, December 6th–22nd; 2004, January 4th–8th; and 2004, January 24th–30th. Ten slightly overlapping fields were used to cover the entire IRAC map of the Perseus Molecular Cloud obtained as part of the *Spitzer* Legacy Project “From Molecular Cores to Planet-forming Disks,” (c2d) (Evans et al. 2003). Two of these fields are centered on the IC 348 and NGC 1333 clusters and are referred as ‘cluster fields’ in the following discussion. Three frames were taken for every pointing of the cluster fields: a 15 sec exposure followed by two 150 sec exposures. For the rest of the fields, only two frames were taken, namely, a 3 sec exposure followed by a 15 sec exposure. From the 3 observing runs, a total of  $\sim 140$  useful data points were obtained for each star of the cluster fields and  $\sim 50$  data points for stars in the rest of the fields. Typical rotation periods of PMS stars range from  $\sim 0.2$  to  $\sim 15$  days.

We tested the range of periods recoverable in our data by inserting sine waves of several different amplitudes into data from non-varying stars of various magnitudes in the IC 348 field. The model variations ranged in period from 0.3 to about 19 days. Using the same detection method in identifying rotation periods in IC 348 PMS stars, recovery rates for the

model variations were about 71% for periods between 0.4 and 0.5 days and 52% for periods between 0.5 and 0.6 days, although most of the periods that were not accurately identified in this regime were a factor of two away from the actual period, which would not affect the overall rotation period distribution significantly. Nearly 100% of the models with periods ranging from 0.6 days and above were correctly identified. Therefore, we conclude that the observations obtained provide both an appropriate sampling rate and baseline to be sensitive to all expected rotation periods.

After standard CCD reductions were performed with the IRAF `imred.ccdred` package, photometry is performed using a combination of the ISIS image subtraction software (Alard & Lupton 1998; Alard 2000) and our own code. After residual images are generated by ISIS, our code measures aperture sums for stars in the residual images and produces light curves measured in percent flux normalized to a reference image. Here we present the rotation periods found in the field covering the IC 348 cluster. Rotation periods for stars in the rest of the Perseus cloud, including those in the cluster NGC 1333, will be presented in a future paper.

### 3.2. Finding the Rotation Periods

To search for periodic signals in the light curves of our targets, we used the standard periodogram technique discussed by Scargle (1982) for analyzing periodic signals of unevenly spaced data and the prescription given by Horne & Baliunas (1986) to select the optimum number of independent frequencies used to inspect the data. The initial period range of the periodogram was set to 0.1–50 days, but, since the number of independent frequencies inspected is heavily weighted toward higher frequencies, low frequencies are not well sampled in this range, which produces a large uncertainty for long periods. For this reason, a new periodogram was produced for every star. In this new periodogram, the shortest period sampled was set to 0.75 times the period found in the first pass. For our data set, the normalized power spectrum (PS) peak of the Scargle periodogram corresponding to a false alarm probability (FAP, as defined by Horne & Baliunas 1986) of 1% is  $\sim 10$ . This threshold corresponds to the 1% probability that a power spectrum peak reaches a given high by pure fluctuations of white, uncorrelated noise, and is clearly too optimistic.

The assumption that the data points are statistically uncorrelated and that noise can be characterized as white is usually not valid for time series photometry of PMS stars (see Rebull 2001, and references therein). The distribution of PS peaks for the entire sample of  $\sim 3600$  stars in the IC 348 field is shown in Figure 1. The left side of the peak can be characterized as a Gaussian centered at 6.4 with a FWHM of 1.5 days. Rightward of the

peak, the PS distribution has a tail corresponding to light curves with real periodic signals combined with spurious signals produced by non-white noise. The shape of the distribution of the PS peaks suggests that periods become unreliable for PS peaks lower than  $\sim 20$ . Since our field contains over 60 stars with known rotation periods from the literature, we can also estimate our PS confidence threshold by plotting the agreement of our periods with published values from Cohen et al. (2004), Littlefair et al. (2005), and Kızıloğlu et al. (2005) as a function of the peak of the PS (Figure 2).

Figure 2 shows that even though some of our periods agree with published values down to a PS peak of  $\sim 10$ , many values start to diverge when the peak is  $\sim 20$ . Above a PS peak of 20, the periods we find disagree with published periods for only 5 objects, labeled A through E in Figures 2 and 3. In what follows we analyze these objects one by one. Object A (ID 91) has a PS peak of 41.9. We find a period of 4.55 days while Kızıloğlu et al. (2005) finds a period of 1.28 days. Figure 3 shows that the period found by Kızıloğlu et al. (2005) can be explained as the beating of our period and a 1 day sampling interval (i.e. a relation of the form  $1/P_{\text{beating}} = \pm 1 \pm (1/P)$ , denoted by the solid line). Object B (ID 102) has a PS peak of 32.5, and we find a rotation period of 8.57 days. Kızıloğlu et al. (2005) assign to this object a rotation period of 32.28 days, which is much longer than the typical rotation periods of PMS stars. Since the period found by them is close to a factor of four larger than our period, it is likely to be an harmonic of the real period.

For object C (ID 98), which has a PS peak of 30.8, we find a period of 19.8 days, while Littlefair et al. (2005) find a period of 13.4 days. Both cases represent an unusually long rotation period and the discrepancy is likely to be due to the increasing uncertainty with increasing period for relatively short observing campaigns. Since our observations span 52 days and Littlefair et al. (2005) observations span only 26 days, our period is more likely to be correct. For object D (ID 123), we find a PS peak of 26.0 and a period of 10.64 days. Kızıloğlu et al. (2005) find a period of 22.51 days, which is also likely to be an harmonic of the real period. Finally, for object E, we find a PS peak of 21.6 and a period of 18.3 days. Littlefair et al. (2005) find a period of 8.4 days. In this case, it is likely that our period is an harmonic of the real period found by the other group. The contamination of rotation-period distributions by harmonics and “beat periods” at the 10% level has already been seen by many groups (e.g. H02 and Lamm et al. 2005) when comparing their results to previously published data. In addition to a change in the beating of a period within the sampling rate (which would be different for each observing run), the observed periods themselves may change between observing runs (as discussed in Rebull 2001) due to the migration of stellar spots in a differentially rotating photosphere. Clearly, the lower the adopted PS threshold, the larger the contamination fraction. For definitiveness, based on Figures 1 through 3 and the above discussion, we adopt a PS peak of 22.0 as the criteria to consider the periodic signal



to be an accurate representation of the rotation period. This corresponds to the highest PS peak of an object showing a significant discrepancy with published periods that we believe is due to our own incorrect period (object E in Figures 2 and 3).

### 3.3. The Rotation Period Distribution

Inspecting the periodograms of the  $\sim 3600$  stars detected in our field, we find 105 objects with PS peaks higher than 22, the adopted detection threshold. Of these 105 objects, only 30 had previously known rotation periods. Thus, we have obtained 75 new rotation periods. Our periods more than double the number of previously known rotation periods in the IC 348 cluster and increase the total number to 143; a comprehensive list of all known stars with periods in IC 348 appears in Table 1. The coordinates of each periodic stars listed are those of the closest counterpart identified in the 2MASS survey. Figure 4 shows the histogram of all the rotation periods listed in Table 1. The period distribution extends to almost 30 days; however, for the rest of the paper, we restrict our analysis to the 132 stars listed in Table 1 with periods shorter than 15 days. We decided to make this cut because stars with periods  $> 15$  days ( $\sim 8\%$  of the total sample) are likely to be more contaminated by harmonics than the rest of of stars (in the previous section we found that periods longer than 15 days account for 3 out the 5 stars with PS peaks larger than 22 which have a period disagreement with previously published values). Also, any MS star contaminating our sample is likely to have a rotation period  $> 15$  days.

### 3.4. The Periodic Sample

The stellar population of IC 348 and its disk properties are very well characterized. Luhman et al. (2003) present a spectroscopic census of the the cluster members. This census is nearly complete within the central  $16' \times 14'$  area of the cluster for stars with spectral types M8 and earlier and yields a sample of 288 objects whose membership has been established based on their proper motions, positions in the H–R diagram,  $A_V$ 's, and spectroscopic signatures of youth. More recently, Lada et al. (2006) present *Spitzer* observations of all the 288 objects identified by Luhman et al. (2003) as IC 348 members. These results are based on the the same IRAC GTO observations we use for disk identification, and will be discussed further in Section 5.1.

Of the 143 periodic stars listed in Table 1, 92 are identified by Luhman et al. (2003) as members of the cluster, and each of them have measured spectral types. We note that the 51

stars in our sample which are *not* identified by Luhman et al. (2003) as IC 348 members fall outside the  $16' \times 14'$  field for which they present a complete membership census. However, Cambr esy et al. (2006) present an extinction map of the IC 348 region and conclude that the cluster extends up to  $25'$  from its center, placing all the objects in our sample within those cluster boundaries. Most of the periodic stars in our sample turned out to be known members of IC 348, while only 8% of all of the stellar light curves we inspected correspond to the 288 known members identified by Luhman et al. (2003). More importantly, none of our periodic stars correspond to any of the 123 targets identified by Luhman et al. (2003) as foreground or background non-members of the cluster. This indicates that periodicity is a very efficient selector for PMS stars, and we conclude that it is therefore likely that most, if not all, of the periodic stars falling outside the region studied by Luhman et al. (2003) are in fact members of the IC 348 cluster.

### 3.5. Mid-IR Observations and Data Reduction

As part of the c2d Legacy Project (Program ID 178), *Spitzer* has mapped 3.8 sq. deg. of the Perseus Molecular Cloud with the Infrared Array Camera (IRAC, 3.6, 4.5, 5.8, and  $8.0 \mu\text{m}$ ) containing the IC 348 cluster and its surroundings. The IRAC maps consist of four dithers of 10.4 sec observations divided into two epochs (i.e. a total of 41.6 sec exposures per pixel) separated by several hours. The second-epoch observations were taken in the High Dynamic Range mode, which includes 0.4 sec observations before the 10.4 sec exposures, allowing photometry of both bright and faint stars at the same time. See Jorgensen et al. (2006) for a detailed discussion of the c2d IRAC observations of the Perseus Molecular Cloud. Also, *Spitzer* has obtained deep observations IC 348 as part of the Guaranteed Time Observer program (GTO) “Deep IRAC imaging of Brown Dwarfs in Star Forming Clusters” (Program ID 36). These observations cover a  $15' \times 15'$  field of view centered in the cluster and consists of two pairs of 8 dithers of 96.8 sec exposures for the 3.6, 4.5, and  $5.8 \mu\text{m}$  observations (1549 sec exposures per pixel). A characteristic of this observing mode splits each  $\sim 100$  sec IRAC4 exposure into two equal exposures. As a result, the  $8.0 \mu\text{m}$  observations consist of four pairs of 8 dithers of 46.8 sec exposures.

The results of the *Spitzer* observations of the entire population of IC 348 members is presented in Lada et al. (2006). For consistency, we processed the Basic Calibrated Data from the GTO program and produced point source catalogs using the c2d pipeline. The c2d pipeline uses the the c2d mosaicking/source extraction software, c2dphot (Harvey et al. 2004), which is based on the mosaicking program APEX developed by the *Spitzer* Science Center and the source extractor Dophot (Schechter et al. 1993). See Evans et al. (2006) for

a detailed description of the c2d data products. We searched the c2d and GTO IRAC point source catalogs and found fluxes for 127 of the 143 objects listed in Table 1 (i.e., 16 of the periodic objects fall outside the c2d/GTO IRAC maps of Perseus).

### 3.6. Complementary data

In addition to the rotation periods and the IRAC photometry, we have collected the following complementary data for our stars in Table 1. First, with the same telescope used to obtain the time series photometry, we obtained RI absolute photometry for our field. We performed PSF fitting photometry with the standard IRAF implementation of the DAOPHOT (Stetson 1987) and used Landolt standards for calibration (Landolt 1992). We report RI data for all but a few stars listed in Table 1 that fall outside the field due to a small pointing error. Also, we have collected the 2MASS J, H and K magnitudes for all but 3 very faint stars. Finally, we have collected all the spectral types available for our sample, covering 92 objects from Luhman et al. (2003). All the complementary data are also listed in Table 1.

## 4. Testing the Disk Regulation Paradigm

### 4.1. Identification and Classification of Mid-IR Excess

In recent *Spitzer* studies of circumstellar disks, different groups adopt different disk identification criteria. An effective and reliable method of disk identification is crucial to this type of survey, especially when dealing with a small sample size, such as is the case with the IC 348 rotation periods. A near-100% recovery of disks with few or no false positives using IRAC photometry is possible. Here we discuss the disk-identification criteria used in two studies particularly relevant to this paper: The study of the correlation between stellar rotation and IRAC excess in Orion (Rebull et al. 2006) and the *Spitzer* observations of all the confirmed members of IC 348 (Lada et al. 2006). Bare stellar photospheres have an IRAC color  $\sim 0.0$ , while stars with an IR excess have positive colors. The broader the color baseline used, the larger the mean IR excess of the stars with disks; therefore, the IRAC color that provides the clearest separation between stars with and without disks is [3.6]–[8.0]. For their study of periodic stars in the ONC, Rebull et al. (2006) adopt the color [3.6]–[8.0]  $> 1.0$  as the criterion for disk identification. This boundary is chosen based on the shape of the [3.6]–[8.0] histogram of their sample, which shows a clear deficit of periodic stars around this color. Lada et al. (2006) use a criterion based on the slope,  $\alpha$ , of a power law fit to the four IRAC

bands. From the comparison to disk models, they identify objects with  $\alpha > -1.8$  as optically thick disks. Based on the predicted slope of an M0 star and the typical uncertainty in the power law fit, they identify objects with  $\alpha < -2.56$  as bare stellar photospheres. Objects with intermediate slopes,  $-2.56 > \alpha > -1.8$ , are termed “anemic disks” and are interpreted as optically thin disks or disks with inner holes.

We find that the disk criteria adopted by the Lada and Rebull groups identify a slightly different set of stars. In this section, we propose alternative disk identification criteria and explore the differences between our criteria and those adopted by the other groups. In order to construct our disk-identification criteria, we first collect IRAC colors for a large sample of PMS stars with high signal to noise ratios (S/N) from the literature. We construct our sample from the classical and weak-lined T Tauri stars (cTTs and wTTs) studied by Hartmann et al. (2005), Lada et al. (2006), Padgett et al. (2006), and Cieza et al. (2006, in prep). To minimize the uncertainties, we restrict the sample to the 435 objects for which reported photometric errors are less than 0.1 mag and explore the location of this sample in different color-color diagrams. We find that the [3.6]–[8.0] *vs.* [3.6]–[5.8] diagram shown in the left panel of Figure 5 provides the best separation of stars with and without a disk. This combination of colors results in a well-defined locus of stellar photospheres and of cTTs wTTs disks. We identify the stars with [3.6]–[8.0]  $> 0.7$  located along the dash-dotted line as stars with disks and stars with [3.6]–[5.8]  $< 0.5$  and [3.6]–[8.0]  $< 0.5$  as diskless stellar photospheres. Only  $\sim 1\%$  of the sample (5/435) have  $0.7 > [3.6] - [8.0] > 0.5$ , where the colors of the weakest disks seem to overlap with the colors of the redder stellar photospheres. We note that the few photospheres slightly redder than the main clump correspond, for the most part, to M2–M6 stars.

Incidentally, a linear fit to the sample of stars with disks yields

$$([3.6] - [8.0])_{\text{DISKS}} = 1.39 \pm 0.05 \times ([3.6] - [5.8])_{\text{DISKS}} + 0.43 \pm 0.03$$

This relationship extends over one magnitude in the [3.6]–[5.8] color and two magnitudes in the [3.6]–[8.0] color with a  $1\sigma$  dispersion of 0.15 mag. The tightness of this *IRAC locus of T Tauri star disks* is comparable to that of the loci of cTTs in the near-IR defined by Meyer et al. (1997). Therefore, one can use this convenient IRAC locus of disks as an initial tool to identify wTTs and cTTs candidates in any IRAC field. One might expect contamination from galaxies with IRAC colors similar to stars in this locus. However, we found that in the fields observed by the Spitzer Wide-area InfraRed Extragalactic survey (SWIRE), only about  $\sim 15\%$  of the objects fell within a  $3\sigma$  distance from this IRAC locus.

In order to compare our disk-identification criteria to those adopted by Lada et al. (2006) and Rebull et al. (2006), we plot the [3.6]–[8.0] *vs.* [3.6]–[5.8] colors reported by the Lada group for their entire sample of IC 348 objects (288 stars) with different symbols, indicating

the classification given in their study (Figure 5, right panel). This figure shows that the disk-identification criterion adopted by Rebull and collaborators (i.e.  $[3.6]-[8.0] > 1.0$ ) selects a sample of stars which has an almost one-to-one correspondence with the objects classified as optically thick disks by the Lada group, meaning the Rebull criterion misses disks with weaker mid-IR signatures. On the other hand, Lada and collaborators classify as anemic disks both objects that belong to our IRAC locus of T Tauri star disks and some objects which have colors consistent with bare stellar photospheres (i.e., the Lada criteria overestimate the number of anemic disks). We believe this is a consequence of adopting criteria for disk identification which are independent of spectral type. In fact, most of the objects classified as anemic disks by Lada et al. (2006) which do not satisfy our disk identification criteria are late M stars. In addition, the scatter in the right panel of Figure 5 is dominated by the photometric error in  $8.0 \mu\text{m}$  fluxes of the faintest stars, which also comprise the handful of objects with nonphysical negative  $[3.6]-[8.0]$  colors.

Figure 6 shows the  $[3.6]-[8.0]$  vs.  $[3.6]-[5.8]$  colors of our periodic sample in IC 348, restricted to the 109 stars in Table 1 with 3.6, 5.8, and  $8.0 \mu\text{m}$  fluxes and periods  $< 15$  days. We find that 40 stars have a color  $[3.6]-[8.0] > 0.7$ , indicating the presence of a disk, and that only 3 stars have borderline colors,  $0.7 > [3.6]-[8.0] > 0.5$ . Two of the objects with intermediate colors (ID= 72 and 111) are faint M4.75–M5 stars; therefore, we classify them as diskless stars. The other object (ID=88) is of unknown spectral type. We searched the catalogs from the c2d Legacy Project and found that this object has a  $24 \mu\text{m}$  flux of 23.1 mJy, which corresponds to a  $24 \mu\text{m}$  excess of over 4 magnitudes. Thus, we classify this object as possessing a disk, leading to a total number of disks in our sample of 41 and a disk fraction of  $38\% \pm 5\%$  (41/109).

Given the fact that only 3 objects in our sample have a somewhat ambiguous disk identification, we estimate our disk census to be both complete and reliable at the  $\sim 97\%$  level. In contrast, Hillenbrand et al. (1998) show that color-color diagrams combining optical and near-IR data can only identify  $< 70\%$  of the accretion disks in a given sample and that this efficiency decreases for very low-mass stars (e.g. spectral types later than M2). Also, *Spitzer* can identify stars with low accretion rates and disks with inner holes which have no near-IR excess (e.g. Padgett et al. 2006), making *Spitzer* data (combined with effective disk-identification criteria, as described above) a more effective tool for disk identification than any ground-based near-IR observations.

Having accurately determined which stars have disks, one can then conduct a comprehensive search for any correlation between stellar rotation period and the presence of a disk. The period distributions for stars with and without a disk are shown in Figure 7, while Figure 8 shows the  $[3.6]-[8.0]$  color as a function of rotation period. The most striking feature of

Figure 7 is that stars with disks show a bimodal distribution even more-clearly defined than that seen in the entire sample. This fact goes directly against the first order prediction of the current disk-locking paradigm in which the bimodal distribution itself is a manifestation of two populations of stars, one with disks (slow rotators) and another without disks (fast rotators). Similarly, Figure 8 shows no evidence of any correlation between period and the *magnitude* of the IR excess. A standard Spearman test yields over an 84% chance that the quantities are completely uncorrelated. However, before drawing any further conclusions from Figures 7 and 8, we would like to explore and attempt to disentangle another variable which has been claimed to correlate with rotation period: Stellar mass.

#### 4.2. Mass Dependence

Following H00, most authors have divided their rotation period distributions into “high mass” and “low mass” stars. The H00 masses come from Hillenbrand (1997) and were obtained using the evolutionary tracks by D98. The  $0.25 M_{\odot}$  division should be regarded as a nominal value throughout the paper since PMS stellar masses are highly model dependent. We point out that D98 models yield systematically lower masses than other widely used evolutionary models such as those presented by Baraffe et al. (1998) and Siess et al. (2000). According to the D98 models, for ages less than several million years, the  $0.25 M_{\odot}$  division corresponds to the M2 spectral type. Therefore, other authors (e.g Rebull 2001) have used spectral type as a proxy for stellar mass. Optical colors ( $R_C-I_C$ ) have also been used to differentiate between low- and high-mass stars (e.g. Lamm et al. 2005).

Ever since a statistically significant number of rotation periods became available, it has been suggested that rotation periods are highly dependent on mass. H00 argued that stars more massive than  $\sim 0.25 M_{\odot}$  show a bimodal distribution, while lower-mass stars show a more uniform distribution and a lack of fast rotators ( $P < 2$  days). H00 attributed the lack of low-mass fast rotators to a deuterium-burning phase that temporarily halts the contraction of low mass stars. However, deeper observations of the ONC (e.g. H02) later showed a large population of fast-rotating, low-mass stars. In fact, H02 argue that low-mass stars rotate significantly faster than high-mass stars and that the period distribution of low-mass stars peaks at  $\sim 2$  days (i.e. the apparent lack of low-mass fast rotators previously reported was a selection effect). Using  $R_C-I_C$  color criteria, Lamm et al. (2005) also find that low-mass ( $R_C-I_C > 1.3$ ) stars rotate, on average, faster than “high” mass ( $R_C-I_C < 1.3$ ) stars. However, other authors have cast doubts on this conclusion. Rebull (2001) finds that the periods of high-mass stars (spectral type earlier than M3) and low-mass stars (spectral types M3 and later) in the Orion Flanking Fields are statistically consistent with each other.

However, as mentioned earlier, Herbst & Mundt (2005) regard the Rebull (2001) sample as too heterogeneous in terms of age for any period dependence on disk properties or mass to be observable.

Naturally, we would like to explore the mass dependence in our period distribution. In order to divide our sample into “high” and “low” mass stars, we take advantage of the large amount of information collected in Table 1. Most of the stars in our sample (92/143, 64%) have spectral types from Luhman et al. (2003). We classify stars with spectral type M2 and later as low-mass stars and stars with spectral types earlier than M2 as high-mass stars. For stars without spectral types, we adopt the following procedure. First, we classified the objects based on their  $[3.6]-[4.5]$  *vs.*  $[3.6]-[8.0]$  colors. Sources with  $[3.6]-[4.5] < 0.2$  and  $[3.6]-[8.0] < 0.5$  are consistent with bare stellar photospheres. For these objects, we obtain photometric approximations of spectral types by fitting the RIJHK and IRAC magnitudes to stellar models of different spectral types corrected for extinction.

The stellar models were constructed as in Cieza et al. (2005), from optical and near-IR broadband colors from Kenyon & Hartmann (1995) tied to IRAC colors based on Kurucz models (Kurucz 1993). We adopt the extinction corrections also listed in Cieza et al. (2005). For stars with  $[3.6]-[4.5] < 0.2$  and  $[3.6]-[8.0] > 0.5$  (e.g. stars without  $4.5 \mu\text{m}$  excess but with significant  $8.0 \mu\text{m}$  excess), we follow the procedure describe above, but without fitting the  $8.0 \mu\text{m}$  or  $5.6 \mu\text{m}$  data points (in practice, the weights of the IRAC data points in the fit are set by the corresponding “excess”). We tested our procedure with 58 stars with spectral types and  $[3.6]-[4.5] < 0.2$  and find that, remarkably, our photometric spectral types typically agree with those reported by Luhman et al. (2003) to within a spectral subtype. Namely,  $\text{MEAN}(\text{Spt}_{\text{Luhman}} - \text{Spt}_{\text{phot}}) = 0.26$  and  $\text{MEAN}(\text{ABS}(\text{Spt}_{\text{Luhman}} - \text{Spt}_{\text{phot}})) = 0.69$ , where one spectral type subclass equals unity and spectral types are ordered from early to late.

Finally, objects with  $[3.6]-[4.5] > 0.2$  and  $[3.6]-[8.0] > 0.5$  are likely to be cTTs with thick inner disks (e.g. Lada et al. 2006). Meyer et al. (1997) show that cTTs occupy a very-well-defined locus in the *dereddened* H–K *vs.* J–H diagram. We take advantage of this fact and estimate the  $A_V$  of the few objects with  $[3.6]-[4.5] < 0.2$  and unknown spectral types by dereddening them to the the locus defined by Meyer et al. (1997). Using the  $A_V$ ’s estimated in this way, we deredden their  $R_C - I_C$  colors. We classified stars with  $(R_C - I_C)_o < 1.3$  as high-mass stars and stars with  $(R_C - I_C)_o > 1.3$  as low-mass stars (where a  $R_C - I_C$  color of 1.3 corresponds to a spectral type of M2). The period distributions for low- and high-mass stars are shown in Figures 9. We find that the period distributions are remarkably similar to those presented by H02 for the heart of the ONC. Stars estimated to be less massive than  $0.25 M_\odot$  show a unimodal distribution dominated by fast rotators ( $P \sim 1-2$  days) and a

tail of slow rotators, while stars estimated to be more massive than  $0.25 M_{\odot}$  show a bimodal distribution with peaks at  $\sim 2$  and  $\sim 8$  days. Thus, our results confirm the strong dependence of stellar rotation on mass, as observed by H02 in the heart of the ONC and by Lamm et al. (2005) in NGC 2264.

As mentioned in section 2, Lamm et al. (2005) find that the peaks in the period distribution observed in NGC 2264 are shifted toward shorter periods with respect to those seen in the ONC. These shifts are interpreted as evidence of angular momentum evolution between the ONC (age  $\sim 1$  Myrs) and NGC 2264 (age  $\sim 2$ – $4$  Myrs). Do we see the same angular momentum evolution between the ONC and IC 348 (age  $\sim 3$  Myrs)? On one hand, the location of the peaks in the period distribution of the high-mass stars in IC 348 suggests that they have spun down with respect to those in the ONC. On the other hand, the median period of the low-mass stars in IC 348 seems to suggest that these stars have spun up with respect to the low-mass stars in the ONC. However, given the size of the sample and the magnitude of the changes, none of the differences are statistically significant.

### 4.3. IR Excess–Rotation Period Correlation?

Taking the low- and high-mass stars separately, is there any evidence that stars with disks rotate slower, as a group, than stars without disks? Given the substantial improvement in the disk identification efficiency using IRAC observations over near-IR indicators, the disk–period correlation reported by H00 and H02, if real, should be readily-detectable in our data. Figure 10 shows the  $[3.6]$ – $[8.0]$  color *vs.* period for both low- and high-mass stars. A standard Spearman test shows that there is a 68% chance that the period of high-mass stars is completely uncorrelated with IR excess. This chance drops to 23% for low-mass stars, but the significance level is not anywhere near the level found by H02 for the correlation between period and (I–K) excess in Orion stars (H02 find that there is a  $10^{-10}$  chance that period and (I–K) excess are uncorrelated quantities). Our results support the claim made by Littlefair et al. (2005) that the correlation between period and (I–K) is a secondary manifestation of the correlation between near-IR excess and mass. Most of the power in the weak correlation between period and IRAC excess comes from the fact that the 5 fastest rotators (all of them low-mass objects) show little or no excess. We discuss this point in Section 5.2.

Low-mass stars show a unimodal distribution peaking at  $\sim 1$ – $2$  days and a tail of slow rotators. According to the disk-braking model, one would expect stars without disks to be concentrated around the 1–2-day peak and stars with disks to be concentrated in the long-period tail. We find no evidence of that being the case. If anything, we find the opposite to be true. The median period of the sample of low mass objects is 3.58 days. The disk fraction



of the objects rotating faster than the median is  $38\% \pm 8\%$  (11/29), while the disk fraction of the objects rotating slower than the median is  $21\% \pm 7\%$  (6/29). High-mass stars show a bimodal distribution peaking at  $\sim 2$  days and  $\sim 8$  days. In the context of the disk-braking model, one would expect, for the most part, stars populating the short-period peak to be objects without disks and the stars populating the long-period peak to be stars with disks. Again, we find no significant evidence for disk braking. We find that  $39\% \pm 10\%$  (9/23) of the high-mass stars rotating faster than the median ( $P = 6.2$  days) have disks, while a marginally higher fraction of stars rotating slower than the median,  $50\% \pm 10\%$  (12/24), have disks.

## 5. Discussion

The fact that we find no evidence for a correlation between period and the presence of IR excess represents a serious challenge to the current paradigm of the evolution of angular momentum of PMS stars, which relies heavily on disk braking to explain the presence of slowly rotating PMS and ZAMS stars. It could be argued that the  $8.0 \mu\text{m}$  excess is *too good* a disk indicator, enabling detection of disks with inner holes too large for the disk to still be locked to the star. However, disk models show that stars with inner holes have lower  $8.0 \mu\text{m}$  excesses than stars with disks extending inward to the dust sublimation temperature (e.g. Padgett et al. (2006) models of wTTs *versus* Cieza et al. (2005) models of cTTs). Therefore, even if a diversity of inner hole sizes were responsible for masking the disk–period correlation in the histograms in Figure 7, one would expect periods to correlate with the *magnitude* of the  $8.0 \mu\text{m}$  excess (one would expect stars with strong  $8.0 \mu\text{m}$  excess to rotate slower than stars with weak or no  $8.0 \mu\text{m}$  excess). As illustrated by Figure 8, we find no evidence of such a correlation either. Throughout the paper, we use the  $8.0 \mu\text{m}$  excess as a disk indicator because, as discussed in Section 4.1, it provides the best separation between stars with and without disks; however, we see no period–IR excess correlation using the excess at any of the IRAC bands as a disk indicator.

There is currently no quantitative theory for disk braking; however, some authors have tried to make some quantitative analysis based on the derived distributions of angular momentum for stars of different ages. Herbst & Mundt (2005) construct the distributions of the specific angular momentum of the ONC, NGC 2264, and a sample of main sequence (MS) stars, combining objects from the Pleiades,  $\alpha$  Per, and the IC 2602 clusters. Specific angular momentum,  $j$ , is obviously a more relevant quantity than period to study the evolution of angular momentum of PMS stars. However, its calculation requires the knowledge of the stellar radius (e.g.  $j \propto R^2/P$ ). To that end, Herbst & Mundt (2005) assume a mean radius of  $2.09 R_{\odot}$  for stars in the ONC and of  $1.7 R_{\odot}$  for stars in NGC 2264. They argue that the

ONC, NGC 2264, and MS clusters represent a clear sequence in the evolution of angular momentum corresponding to 3 different ages, nominally: 1, 2 and 50 Myrs.

Herbst & Mundt (2005) suggest that the broad distribution of angular momentum observed in their sample of MS stars can be explained by assuming that 40–50% of the PMS stars conserve angular momentum when they contract while the remainder of the stars, *which should already be slow rotators by the ages of the ONC and NGC 2264*, must stay disk-locked for up to 5 Myrs in order to account for the slow rotators in the ZAMS sample (this is consistent with the findings of (Rebull et al. 2004)). Were this the case, we should see strong evidence for disk locking in our sample of PMS stars with rotation periods and IR-excess measurements. Since we see no such evidence, our results are inconsistent with the Herbst & Mundt (2005) claim, unless, for some reason, our sample is severely biased against disk-locked stars. We investigate the possibility of such a bias in the next section.

### 5.1. Sample bias?

A critical point regarding the validity of the conclusions of this paper is to what degree our sample of stars with rotation periods is representative of the entire population of IC 348 members. Fortunately, the stellar population of IC 348 and its disk properties are very well characterized. As discussed in Section 3.4, Luhman et al. (2003) present a detailed spectroscopic census of IC 348 cluster members, complete for spectral type M8 and earlier, and Lada et al. (2006) have recently presented *Spitzer* observations of all the 288 objects identified by Luhman et al. (2003) as IC 348 members. Because the Lada results are based on the the same IRAC GTO observations we use for disk identification, they provide a perfect test to investigate the possibility of any strong disk fraction bias in our sample of IC 348 members with rotation periods with respect to the entire cluster population.

Cohen et al. (2004) argue that, since none of the 28 periods they report correspond to known cTTs, rotation period samples are heavily biased against accreting objects, where disk braking is more likely to occur. In contrast, Littlefair et al. (2005) report that 43% of their periods correspond to cTTs, a result which is not significantly different from the overall cTTs fraction among IC 348 members ( $\sim 40\%$ ). They argue that the drastic improvement in the efficiency for obtaining rotation periods of cTTs in their work with respect to the Cohen et al. (2004) results is due to the high sampling density of their observations; cTTs are highly non-periodic on time scales larger than a few days or weeks. Cohen et al. (2004) periods come from an observing campaign spanning several years with a very low temporal density, while Littlefair et al. (2005) observations come from a 26-night campaign with a typical sampling rate of one frame every 10 minutes. Our observations also had very high

temporal density and yield a cTTs fraction of  $\sim 40\%$ .

Using the same disk identification criteria ( $[3.6]-[8.0] > 0.7$ ) for the entire sample of IC 348 members studied by Lada et al. (2006) and for the periodic sample listed in Table 1, we find the disk fractions to be the same within statistical errors,  $41\% \pm 2.7\%$  vs.  $38\% \pm 5\%$ , respectively. Since there is no evidence that our sample is biased against stars with disks, we conclude that our sample of stars with rotation periods is representative of the entire population of IC 348 members in terms of their disk properties. Rebull et al. (2006) reach the same conclusion for the stars in Orion by noting that the  $[3.6]-[8.0]$  color distribution of the periodic stars is statistically indistinguishable from that of the entire population of Orion members. Therefore, we argue that it is very unlikely that the lack of correlation between rotation period and IR excess is due to a bias in the disk properties of our sample.

## 5.2. Previous Spitzer Results and Very Fast Rotators

Previous to this paper, the analysis of the periodic stars in Orion by Rebull et al. (2006) is the only study that combines rotation periods and *Spitzer* observations. They study a sample of 464 stars with known rotation periods and  $[3.6]-[8.0]$  colors. They note that the cumulative distribution function of periods for stars with disks (i.e.,  $[3.6]-[8.0] > 1$ ) shows an inflection point around 1.8 days. Based on this inflection point, they divide their sample into “short” and “long” period stars. They find that stars with short periods are *significantly* less likely to have a disk than stars with long periods. However, they also find that for periods  $> 1.8$  days, the period distributions for stars with and without disks are statistically *indistinguishable*.

Our results are consistent with those of the Rebull group. Although at a lower significance level, due to the smaller size of our sample, our results also suggest that there is a significant decrease in the disk fraction at very short periods. As mentioned in Section 4.3, most of the power in the weak correlation between period and  $8.0\ \mu\text{m}$  excess for low-mass stars in IC 348 arises from the fact that the 5 fastest rotators ( $P < 1.2$  days) have very little or no excess at all. Using the same disk identification criteria ( $[3.6]-[8.0] > 1.0$ ) and definition of “short” and “long” period stars adopted by Rebull et al. (2006), we find that only  $12\% \pm 7\%$  (2/16) of the short-period ( $P < 1.8$  d) stars in IC 348 have a disk, while  $33\% \pm 5\%$  (31/93) of the long-period ( $P > 1.8$  d) stars have a disk. These disk fractions are consistent with those seen in the ONC by Rebull and collaborators.

The low disk fraction of fast rotators is evident in Figure 11, where we plot angular velocity ( $2\pi P^{-1}$ ) as a function of  $[3.6]-[8.0]$  color in order to better resolve the distribution

of IR excesses at short periods. At first glance, the upper envelope of the IR excess seems to correlate with angular velocity. However, that is mostly due to the fact that most of the objects are concentrated at low angular velocity. The objects plotted in Figure 11 are the same objects plotted in Figure 10. From a statistical point of view, the significance in the correlation between period and IR excess is *identical* to that of the correlation between angular velocity and IR excess. The fact that very fast rotators tend to have little or no excess is also confirmed to a high level of significance by a preliminary analysis of *Spitzer* data on NGC 2264, which will be fully analyzed and presented in a follow-up paper (Cieza et al. 2007, Paper II).

The low disk frequency of very fast rotators is the only feature of our sample that could *potentially* be interpreted as an evidence for disk braking. In the context of disk braking, stars that lost their disks very early in their evolution are expected to become very fast rotators. The main challenge for disk braking seems to be the large number of slow rotators without a disk. Qualitatively, it has been proposed that the large number of slow rotators that show no evidence of a disk are objects that have recently lost their disks and have not had enough time to spin up considerably (e.g. H02, Rebull et al. 2005, 2006). This scenario would require the spin-up timescale for the stars in the sample to be significantly longer than the transition timescale from a massive inner disk capable of disk braking to a disk tenuous enough to remain undetectable at IRAC wavelengths. However, we note that the population of fast rotators ( $P < 1.8$  d) represents only a small fraction ( $\sim 15\%$ ) of the entire sample of stars with rotation periods in both IC 348 and the ONC. In other words, the vast majority of stars with rotation periods, about 85% in each cluster, shows no correlation between their rotation period and the presence of a disk. This casts serious doubts on the explanation discussed by the three groups mentioned above that the large population of slow rotators with no mid-IR excess is populated by stars which have just lost their disks. This would require  $\sim 50\%$  of the entire sample of periodic stars in each cluster to fall into this special regime. A more quantitative test of this scenario is underway and will be presented in Paper II.

Furthermore, we note that there are other possible explanations for the low disk fraction of very fast rotators besides disk braking. For instance, if the disk fraction of low mass stars, which tend to be very fast rotators, is significantly lower than that of higher mass stars, then an overall lower disk fraction of fast rotators is expected. Results from Lada et al. (2006) suggest that this might be the case. They find that the fraction of *optically thick* disks decreases from  $47\% \pm 12\%$  for K6–M2 stars to  $28\% \pm 5\%$  for M2–M6 stars. As discussed in Section 4.1 and illustrated by Figure 5, the criteria adopted by Rebull et al. (2006) for disk identification selects a sample which has almost a one-to-one correlation with the objects classified as optically thick disks by the Lada group. Also, as noted by Rebull and

collaborators, an overabundance of close binaries among very fast rotators could account for their low disk fraction.

### 5.3. Are our results inconsistent with disk-braking?

How significant is the fact that we see no clear evidence of a correlation between rotation period and IR excess (with the exception of the fastest rotators as mentioned in the previous section)? Is the lack of evidence enough to exclude disk braking as a viable model? At least one line of argument suggests the contrary. Rebull et al. (2004) perform a series of Monte Carlo simulations of the evolution of rotation periods for stars in the context of the disk-braking model. They assume a Gaussian initial period distribution centered at 8 days with a  $1\sigma$  dispersion of 4 days. In their models, they have a population of disk-locked stars that contract at constant angular velocity and a disk-free population which spins up as  $P \propto t^{-2/3}$  (appropriate for stars on convective tracks). The only free variables in their model relate to the fraction of disk-locked stars as a function of time.

After running a series of simulations, they perform K–S tests to constrain the circumstances under which a statistically significant correlation between period and IR excess would be expected. They conclude, given a broad distribution of initial periods, that the observational signatures of disk braking are much less conspicuous than is usually assumed, *even with a perfect knowledge of which stars have a disk*. They find that, unless the sample is very large ( $> 500$ ), the populations of stars with and without disks only become statistically different if a relatively large fraction ( $\sim 30\%$ ) of the stars is released from their disks at an age  $< 1$  Myr. This is because the effect of disk locking is most important when the stars undergo rapid contraction at very young ages and becomes much less important later on as the contraction rate decreases. Furthermore, the Rebull et al. (2004) simulations can produce both a unimodal distribution of periods similar to the one seen in low-mass stars in IC 348 and a bimodal distribution similar to that of the higher-mass stars.

These caveats prevent us from drawing any categorical conclusion regarding the general validity of the disk-locking scenario. There is currently no alternative model to disk braking to explain the evolution of angular momentum of PMS stars, and there is some strong evidence that magnetic star–disk interaction actually occurs in early stages of the evolution of PMS stars (e.g. the presence of highly collimated jets in cTTs and deeply embedded objects). Therefore, we argue that a much more rigorous and quantitative analysis than that presented herein is required before the model can be regarded as inconsistent with the observational data. The fundamental question now becomes whether disk braking, which seems to be required to explain the angular momentum loss experienced by a large fraction

of PMS stars between the birthline and the ZAMS, can occur early on in the evolution of PMS stars without leaving a clear correlation between rotation period and IR excess at the ages of clusters like IC 348.

To address this question, a more rigorous model than the one used by Rebull et al. (2004) could be created to investigate the range of disk-braking parameters (disk-braking efficiency and the fraction of regulated stars as a function of time) which would be allowed by the observed period distribution of stars with and without disks in clusters like IC 348, NGC 2264, and the ONC. For instance, instead of starting from an initial distribution of rotation periods, one could use specific angular momentum, which is more physically meaningful and removes most of the dependence on the initial masses of the objects from the results. The initial angular momentum of the cluster can be constrained by the objects with a maximum current angular momentum (since they will have evolved with the lowest angular momentum loss). It would also be beneficial to incorporate into the models an age spread in the stellar population and observational constraints on the disk fraction as a function of age. Finally, instead of assuming a  $P \propto t^{-2/3}$  relation for all unregulated stars, the evolution of their periods can be calculated from the predicted evolution of their radii by theoretical evolutionary tracks.

In Paper II, we plan to perform Monte Carlo simulations to determine what initial conditions and disk-braking parameters might lead to the current lack of a correlation between rotation period and IR excess in PMS stars. We will use models similar to Rebull et al. (2004) with the improvements mentioned above to perform an analysis of the IC 348 cluster, using data presented in Table 1, and NGC 2264 and the ONC, combining *Spitzer* archival data and periods published in the literature.

## 6. Summary and Conclusions

We have obtained time series photometry of the young stellar cluster IC 348 and measured 75 new rotation periods. Our results increase the total number of known rotation periods in the cluster to 143. We combined all published rotation periods in IC 348 with *Spitzer* photometry (3.6, 4.5, 5.8, and 8.0  $\mu\text{m}$ ) in order to test the disk braking paradigm, constructing a new, more reliable set of criteria for disk identification with IRAC data.

We find that the IC 348 rotation period distribution resembles that seen in the heart of the ONC: Stars estimated to be less massive than  $0.25 M_{\odot}$  show a unimodal distribution dominated by fast rotators ( $P \sim 1\text{--}2$  days) and a tail of slow rotators, while stars estimated to be more massive than  $0.25 M_{\odot}$  show a bimodal distribution with peaks at  $\sim 2$  and  $\sim 8$  days. We find no evidence that the tail of slow rotators in low-mass stars or the long-period

peak of high-mass stars are preferentially populated by stars with disks, a correlation which is predicted by the current disk-braking paradigm. Also, we find no significant correlation between period and the *magnitude* of the IR excess, regardless of the mass range considered.

Given the large improvement of IRAC observations over near-IR disk indicators, our results support the claim made by Littlefair et al. (2005) that the correlation between period and (I–K) excess reported by several authors is a secondary manifestation of the correlation between near-IR excess and mass. We find that the disk properties of our sample are indistinguishable from the disk properties of the cluster as a whole and conclude that it is very unlikely that the lack of a correlation between rotation period and IR excess is due to a bias in the disk properties of our sample. Finally, we find some indication that the disk fraction might decrease significantly in stars with very short periods ( $P \lesssim 1.2$  days). The fact that very fast rotators tend to have little or no excess has already been shown by Rebull et al. (2005) for stars in the ONC and has been confirmed by a preliminary analysis of our ongoing work with objects in NGC 2264. The low disk fraction of these very fast rotators is the only feature of our sample that could *potentially* be interpreted as an evidence for disk braking.

However, the lack of evidence for disk braking (in the form of a correlation between PMS stellar rotation periods and IR excess) in all but the fastest rotators is not enough to rule out disk braking in PMS stars. As shown by Rebull et al. (2004), current observational signatures of disk braking may be hidden by an initial large distribution of rotation periods in PMS stars. Because there is currently no alternative mechanism for angular momentum loss in PMS stars and because there is evidence for star–disk interaction in very young stellar objects, a rigorous quantitative analysis of the effects of disk-braking parameters on current observational signatures is required to determine whether disk-braking may indeed play a significant role in the angular momentum evolution of these stars. Simulations similar to those run by Rebull et al. (2004), with the improvements suggested in Section 5.3 of this paper, can further constrain the importance of disk braking in the evolution of PMS stars. We are in the process of testing such models and will present our results in a follow-up paper.

We would like to thank the referee for the close reading of the paper. We thank Luisa Rebull and Deborah Padgett for their detailed suggestions. We also thank Paul Harvey, Daniel Jaffe and Neal Evans for their useful comments. We thank Judit Ries for obtaining R and I images and standards for absolute photometry. We also thank Luisa Rebull for providing a preprint of the paper Rebull et al. (2005) prior to publication. Support for this work, part of the Spitzer Legacy Science Program, was provided by NASA through contract 1224608 issued by the Jet Propulsion Laboratory, California Institute of Technology, under NASA contract 1407. This publication makes use of data products from the Two Micron All Sky Survey, which is a joint project of the University of Massachusetts and the Infrared

Processing and Analysis Center funded by NASA and the National Science Foundation.

## REFERENCES

- Alard, C. 2000, *A&AS*, 144, 363
- Alard, C., & Lupton, R. H. 1998, *ApJ*, 503, 325
- Attridge, J. M., & Herbst, W. 1992, *ApJ*, 398, L61
- Baraffe, I., Chabrier, G., Allard, F., & Hauschildt, P. H. 1998, *A&A*, 337, 403
- Cambrésy, L., Petropoulou, V., Kontizas, M., & Kontizas, E. 2006, *A&A*, 445, 999
- Cieza, L. A., Kessler-Silacci, J. E., Jaffe, D. T., Harvey, P. M., & Evans, N. J. 2005, *ApJ*, 635, 422
- Claver, C. F. 1992, *Bulletin of the American Astronomical Society*, 24, 1282
- Cohen, R. E., Herbst, W., & Williams, E. C. 2004, *AJ*, 127, 1602
- Covey, K. R., Greene, T. P., Doppmann, G. W., & Lada, C. J. 2005, *AJ*, 129, 2765
- D’Antona, F., & Mazzitelli, I. 1994, *ApJS*, 90, 467
- D’Antona, F., & Mazzitelli, I. 1998, in *ASP Conf. Ser. 134: Brown Dwarfs and Extrasolar Planets*, 442–+, [D94]
- Evans, N. J., Allen, L. E., Blake, G. A., Boogert, A. C. A., Bourke, T., Harvey, P. M., Kessler, J. E., Koerner, D. W., Lee, C. W., Mundy, L. G., Myers, P. C., Padgett, D. L., Pontoppidan, K., Sargent, A. I., Stapelfeldt, K. R., van Dishoeck, E. F., Young, C. H., & Young, K. E. 2003, *PASP*, 115, 965
- Evans, N. J., Harvey, P. M., Dunham, M. M., Mundy, L. G., Lai, S., Chapman, N., Huard, T., Brooke, T. Y., & Koerner, D. W. 2006, *Delivery of Data from the c2d Legacy Project: IRAC and MIPS (Pasadena,SSC)*, Pasadena, SSC, <http://ssc.spitzer.caltech.edu/legacy/original.html>
- Hartmann, L., Megeath, S. T., Allen, L., Luhman, K., Calvet, N., D’Alessio, P., Franco-Hernandez, R., & Fazio, G. 2005, *ApJ*, 629, 881
- Harvey, P., Cieza, L., Spiesman, W., & c2d Team. 2004, *American Astronomical Society Meeting Abstracts*, 204,



- Herbst, W., Bailer-Jones, C. A. L., Mundt, R., Meisenheimer, K., & Wackermann, R. 2002, *A&A*, 396, 513
- Herbst, W., Maley, J. A., & Williams, E. C. 2000, *AJ*, 120, 349
- Herbst, W., & Mundt, R. 2005, *ApJ*, 633, 967
- Hillenbrand, L. A. 1997, *AJ*, 113, 1733
- Hillenbrand, L. A., Strom, S. E., Calvet, N., Merrill, K. M., Gatley, I., Makidon, R. B., Meyer, M. R., & Skrutskie, M. F. 1998, *AJ*, 116, 1816
- Horne, J. H., & Baliunas, S. L. 1986, *ApJ*, 302, 757
- Jorgensen, J. K., Harvey, P. M., Evans, N. J., Huard, T. L., Allen, L. E., Porras, A., Blake, G. A., Bourke, T. L., Chapman, N., Cieza, L., Koerner, D. W., Lai, S.-P., Mundy, L. G., Myers, P. C., Padgett, D. L., Rebull, L., Sargent, A. I., Spiesman, W., Stapelfeldt, K. R., van Dishoeck, E. F., Wahhaj, Z., & Young, K. E. 2006, *ArXiv Astrophysics e-prints*
- Kenyon, S. J., & Hartmann, L. 1995, *ApJS*, 101, 117
- Kızıloğlu, Ü., Kızıloğlu, N., & Baykal, A. 2005, *AJ*, 130, 2766
- Königl, A. 1991, *ApJ*, 370, L39
- Kurucz, R. L. 1993, *VizieR Online Data Catalog*, 6039, 0
- Lada, C. J., Muench, A. A., Luhman, K. L., Allen, L., Hartmann, L., Megeath, T., Myers, P., Fazio, G., Wood, K., Muzerolle, J., Rieke, G., Siegler, N., & Young, E. 2006, *AJ*, 131, 1574
- Lamm, M. H., Mundt, R., Bailer-Jones, C. A. L., & Herbst, W. 2005, *A&A*, 430, 1005
- Landolt, A. U. 1992, *AJ*, 104, 340
- Littlefair, S. P., Naylor, T., Burningham, B., & Jeffries, R. D. 2005, *MNRAS*, 358, 341
- Luhman, K. L., Stauffer, J. R., Muench, A. A., Rieke, G. H., Lada, E. A., Bouvier, J., & Lada, C. J. 2003, *ApJ*, 593, 1093
- Makidon, R. B., Rebull, L. M., Strom, S. E., Adams, M. T., & Patten, B. M. 2004, *AJ*, 127, 2228
- Meyer, M. R., Calvet, N., & Hillenbrand, L. A. 1997, *AJ*, 114, 288

- Padgett, D. L., Cieza, L., Stapelfeldt, K. R., Evans, N. J., Koerner, D., Sargent, A., Fukagawa, M., van Dishoek, E. F., Augereau, J., Allen, L., Blake, G., Brooke, T., Chapman, N., Harvey, P., Porras, A., Lai, S., Mundy, L., Myers, P. C., Spiesman, W., & Wahhaj, Z. 2006, astro-ph/0603370
- Rebull, L. M. 2001, AJ, 121, 1676
- Rebull, L. M., Stauffer, J. R., Megeath, S. T., Hora, J. L., & Hartmann, L. 2006, astro-ph/0604104, ApJ– in press
- Rebull, L. M., Stauffer, J. R., Megeath, T., Hora, J., & Hartmann, L. 2005, in Protostars and Planets V, Proceedings of the Conference held October 24-28, 2005, in Hilton Waikoloa Village, Hawai'i. LPI Contribution No. 1286., p.8264, 8264–+
- Rebull, L. M., Wolff, S. C., & Strom, S. E. 2004, AJ, 127, 1029
- Scargle, J. D. 1982, ApJ, 263, 835
- Schechter, P. L., Mateo, M., & Saha, A. 1993, PASP, 105, 1342
- Shu, F., Najita, J., Ostriker, E., Wilkin, F., Ruden, S., & Lizano, S. 1994, ApJ, 429, 781
- Shu, F. H., Najita, J. R., Shang, H., & Li, Z.-Y. 2000, Protostars and Planets IV, 789
- Siess, L., Dufour, E., & Forestini, M. 2000, A&A, 358, 593
- Stassun, K. G., Mathieu, R. D., Mazeh, T., & Vrba, F. J. 1999, AJ, 117, 2941
- Stassun, K. G., & Terndrup, D. 2003, PASP, 115, 505
- Stetson, P. B. 1987, PASP, 99, 191

Table 1. Periodic Sample in IC 348

ID	Ra	Dec	P	PS	$Ref_P$	SpT	$R_C$	$I_C$	J	H	$K_S$	[3.6]	[3.6] error	[4.5]	[4.5] error	[5.8]	[5.8] error	[8.0]	[8.0] error
	(deg)	(deg)	(days)	<sup>1</sup>	<sup>2</sup>		<sup>3</sup>		(mag)						(mJy)				
1	55.5847	32.0919	7.7	44	1	—	—	—	13.04	11.96	11.47	1.18e+01	1.00e-01	9.33e+00	8.22e-02	7.48e+00	6.35e-02	9.03e+00	6.65e-02
2	55.6078	32.3506	17.7	61	1	—	16.74	15.30	13.29	12.32	12.00	—	—	—	—	—	—	—	—
3	55.6177	32.5133	4.3	47	1	—	16.78	15.25	13.18	12.31	11.99	—	—	—	—	—	—	—	—
4	55.6257	32.2471	26.9	24	1	—	17.29	16.30	14.64	13.88	13.62	—	—	—	—	—	—	—	—
5	55.6340	32.4914	2.3	30	1	—	14.51	13.60	12.33	11.67	11.45	—	—	—	—	—	—	—	—
6	55.6467	32.5651	0.2	35	1	—	16.12	15.42	14.63	14.24	14.03	—	—	—	—	—	—	—	—
7	55.6486	32.2888	1.2	43	1	—	15.89	15.02	13.84	13.14	12.95	—	—	—	—	—	—	—	—
8	55.6698	32.5729	5.8	45	1	—	—	—	13.34	12.45	12.11	—	—	—	—	—	—	—	—
9	55.6703	32.2263	0.5	30	1	—	16.81	15.07	12.75	11.85	11.52	9.55e+00	9.10e-02	—	—	4.58e+00	5.27e-02	—	—
10	55.6817	31.9875	2.2	60	1	—	15.03	13.76	11.79	10.85	10.53	2.22e+01	1.77e-01	1.40e+01	9.42e-02	9.37e+00	5.66e-02	5.36e+00	5.31e-02
11	55.7311	31.9534	1.9	26	1	—	15.90	14.67	13.28	12.54	12.29	3.95e+00	3.21e-02	2.56e+00	2.26e-02	1.79e+00	2.79e-02	9.82e-01	2.73e-02
12	55.7332	31.9783	22.1	29	1	—	—	—	10.55	9.73	9.02	3.84e+02	5.69e+00	3.23e+02	5.02e+00	3.69e+02	3.62e+00	4.88e+02	4.60e+00
13	55.7589	32.1243	17.3	31	1	—	17.20	15.30	12.83	12.05	11.69	8.59e+00	1.06e-01	6.00e+00	6.94e-02	3.79e+00	5.15e-02	2.12e+00	3.35e-02
14	55.7794	32.1718	6.2	55	1	—	16.22	14.79	12.71	11.71	11.37	1.00e+01	6.95e-02	—	—	4.43e+00	4.06e-02	—	—
15	55.7944	32.5923	6.0	34	1	—	16.44	14.98	12.98	12.04	11.71	—	—	—	—	—	—	—	—
16	55.7981	32.4422	7.5	23	1	—	16.79	15.79	14.33	13.57	13.35	1.52e+00	2.52e-02	1.01e+00	1.39e-02	6.56e-01	2.93e-02	3.35e-01	3.20e-02
17	55.8014	32.5698	0.2	23	1	—	16.14	15.20	14.35	13.75	13.56	—	—	—	—	—	—	—	—
18	55.8072	32.0125	7.8	24	1	—	23.28	19.96	14.26	12.57	11.76	1.26e+01	1.02e-01	1.12e+01	9.15e-02	1.10e+01	8.25e-02	1.32e+01	9.20e-02
19	55.8482	32.2072	3.0	36	1	—	18.84	16.79	14.09	13.15	12.72	4.16e+00	5.29e-02	3.26e+00	3.85e-02	2.82e+00	3.71e-02	2.30e+00	3.73e-02
20	55.8516	32.6421	1.3	54	1	—	16.13	14.56	12.25	11.28	10.92	—	—	—	—	—	—	—	—
21	55.8675	32.0331	8.8	30	1	—	14.94	13.61	11.76	10.72	10.11	4.45e+01	9.46e-01	5.06e+01	5.65e-01	3.85e+01	2.95e-01	3.35e+01	2.40e-01
22	55.8875	32.4674	12.2	27	1	—	17.47	15.81	13.44	12.42	12.08	5.32e+00	1.21e-01	3.52e+00	3.59e-02	2.54e+00	7.28e-02	1.31e+00	4.10e-02
23	55.9382	32.0663	27.6	52	1	—	19.29	17.70	13.78	12.15	11.01	2.35e+01	5.18e+00	1.45e+02	2.57e+00	6.61e+01	1.54e+00	1.03e+02	2.04e+00
24	55.9495	32.2991	9.8	54	1	—	15.79	14.44	12.59	11.68	11.39	9.19e+00	1.46e-01	6.21e+00	7.46e-02	4.28e+00	4.46e-02	2.48e+00	3.31e-02
25	55.9532	32.1259	20.3	27	1	M1.5	15.44	14.16	12.43	11.65	11.37	9.01e+00	1.79e-01	6.60e+00	7.88e-02	4.12e+00	5.04e-02	2.31e+00	4.18e-02
26	55.9534	32.2643	2.9	46	1	—	17.02	15.32	13.01	12.14	11.78	8.50e+00	1.52e-01	8.54e+00	9.87e-02	8.40e+00	7.56e-02	1.04e+01	7.31e-02
27	55.9558	32.1777	13.1	44	1	M3.5	16.36	14.76	12.68	11.85	11.56	7.51e+00	1.14e-01	5.42e+00	6.95e-02	3.55e+00	4.44e-02	2.12e+00	4.02e-02
28	55.9642	32.5302	3.8	60	1	—	15.62	14.18	12.03	11.12	10.80	—	—	—	—	—	—	—	—
29	55.9802	31.9256	9.6	26	1	—	20.92	18.30	14.22	12.31	11.39	2.35e+01	4.41e-01	2.18e+01	2.00e-01	1.80e+01	1.42e-01	1.19e+01	8.50e-02
30	55.9843	32.5050	8.1	52	1	—	15.89	14.51	12.49	11.62	11.33	—	—	—	—	—	—	—	—
31	55.9940	32.2910	12.8	26	1	—	15.85	14.36	12.05	11.12	10.66	3.06e+01	4.63e-01	2.18e+01	4.05e-01	2.06e+01	1.60e-01	2.43e+01	1.70e-01
32	55.9962	32.2392	17.7	28	1	—	17.27	15.82	13.49	12.29	11.39	1.31e+01	2.03e-01	1.40e+01	1.76e-01	1.19e+01	9.46e-02	1.26e+01	9.91e-02
33	55.9981	32.2653	7.6	39	1	—	16.96	15.43	13.06	11.99	11.69	7.19e+00	1.24e-01	4.91e+00	5.29e-02	3.42e+00	4.47e-02	1.94e+00	3.30e-02
34	55.9988	32.2341	14.0	63	1,2	M0.75	15.50	14.19	12.30	11.40	11.06	1.29e+01	1.97e-01	8.97e+00	9.60e-02	6.17e+00	6.52e-02	3.43e+00	5.81e-02
35	56.0090	32.3278	6.2	63	1	—	15.73	14.41	12.51	11.64	11.38	8.84e+00	1.47e-01	6.48e+00	7.87e-02	4.48e+00	3.95e-02	2.62e+00	3.43e-02
36	56.0177	32.2305	1.2	32	1	M4.75	—	—	12.61	11.76	11.41	9.73e+00	1.41e-01	7.41e+00	8.13e-02	4.96e+00	4.95e-02	3.05e+00	5.64e-02
37	56.0283	32.1317	1.3	23	1	M4.25	17.27	15.48	13.03	12.14	11.75	1.01e+01	1.73e-01	8.91e+00	1.05e-01	7.53e+00	8.79e-02	8.11e+00	1.05e-01
38	56.0422	32.0679	2.2	—	3	M5.75	18.25	16.14	13.22	12.41	11.93	8.72e+00	1.14e-01	8.23e+00	8.07e-02	7.25e+00	1.17e-01	7.28e+00	1.22e-01
39	56.0468	32.1378	13.0	—	3	M5.25	17.38	15.39	12.84	12.09	11.75	7.36e+00	1.05e-01	5.35e+00	6.98e-02	3.72e+00	5.52e-02	2.27e+00	6.96e-02
40	56.0469	32.1034	9.1	29	1,2,3,4	M0	15.72	14.34	12.42	11.44	11.16	1.12e+01	1.41e-01	7.35e+00	8.22e-02	5.19e+00	7.27e-02	2.75e+00	7.99e-02
41	56.0476	32.3278	0.8	42	1,2	M3	16.13	14.65	12.56	11.78	11.51	8.94e+00	1.32e-01	6.19e+00	6.99e-02	4.51e+00	4.54e-02	2.42e+00	3.28e-02
42	56.0574	31.9263	8.3	39	1	—	19.31	17.13	13.68	12.19	11.64	1.14e+01	2.12e-01	7.98e+00	2.19e-01	5.13e+00	6.85e-02	3.64e+00	9.47e-02
43	56.0649	32.1561	0.6	—	3,	M7.5	20.94	18.18	14.59	13.78	13.30	2.11e+00	2.42e-02	1.52e+00	1.78e-02	1.11e-01	5.27e-02	4.77e-01	1.96e-02
44	56.0654	32.5245	13.7	44	1	—	14.21	13.07	11.72	10.98	10.75	—	—	—	—	—	—	—	—
45	56.0684	32.1653	3.0	33	1,2,3,4	K0	—	—	11.32	10.58	10.38	2.06e+01	2.90e-01	1.36e+01	1.54e-01	9.46e+00	8.43e-02	5.40e+00	7.21e-02
46	56.0746	32.2056	4.5	29	1	M2.5	15.59	14.10	12.16	11.35	11.07	1.17e+01	1.86e-01	8.08e+00	9.06e-02	5.55e+00	5.84e-02	3.06e+00	5.62e-02
47	56.0758	32.1665	2.7	27	1	M4.25	17.87	15.85	13.21	12.27	11.87	7.07e+00	1.09e-01	6.09e+00	7.55e-02	4.88e+00	5.76e-02	4.04e+00	6.86e-02
48	56.0761	32.1257	2.2	—	3	M4.75	18.27	16.30	—	—	—	3.74e+00	4.99e-02	2.79e+00	3.65e-02	1.94e+00	4.44e-02	2.00e+00	5.69e-02
49	56.0801	32.1262	7.6	—	4	M3.75	—	—	—	—	—	1.50e+01	2.29e-01	1.28e+01	1.40e-01	1.16e+01	1.53e-01	1.28e+01	1.42e-01
50	56.0834	32.1127	8.6	—	3,4	M3.5	17.77	16.04	13.58	12.61	12.23	4.66e+00	6.74e-02	3.41e+00	3.37e-02	2.18e+00	4.54e-02	8.11e-01	3.81e-02

Table 1—Continued

ID	Ra	Dec	P	PS	$RefP^2$	SpT	$R_C^3$	$I_C$	J	H	$K_S$	[3.6]	[3.6] error	[4.5]	[4.5] error	[5.8]	[5.8] error	[8.0]	[8.0] error
	(deg)	(deg)	(days)						(mag)						(mJy)				
51	56.0841	32.1491	2.2	—	3	M2	16.76	15.03	12.70	11.79	11.41	1.01e+01	1.69e-01	9.42e+00	1.03e-01	7.79e+00	9.73e-02	7.59e+00	1.51e-01
52	56.0843	32.5063	2.8	45	1	—	17.11	15.42	13.13	12.20	11.85	7.23e+00	7.55e-02	4.77e+00	7.92e-02	3.20e+00	4.29e-02	1.81e+00	5.97e-02
53	56.0857	32.4610	4.8	51	1	—	17.66	15.79	13.23	12.37	12.01	6.86e+00	9.46e-02	4.49e+00	5.25e-02	2.87e+00	5.34e-02	1.54e+00	4.43e-02
54	56.0886	32.0840	6.9	54	1,3	M2.5	16.82	15.17	12.74	11.73	11.40	9.64e+00	1.35e-01	7.12e+00	7.44e-02	4.79e+00	8.04e-02	2.20e+00	7.35e-02
55	56.0886	32.2103	2.3	30	1	M4.75	17.41	15.71	13.70	12.92	12.51	4.90e+00	5.86e-02	4.30e+00	3.88e-02	3.50e+00	3.99e-02	2.71e+00	6.23e-02
56	56.0898	32.1715	7.0	60	1,2,3,4	M1.5	16.20	14.71	12.62	11.66	11.35	1.02e+01	1.13e-01	7.13e+00	6.83e-02	4.88e+00	5.12e-02	2.68e+00	3.12e-02
57	56.0903	32.1069	8.4	—	2,4	M2.75	16.21	14.65	12.54	11.60	11.31	9.91e+00	1.40e-01	6.67e+00	8.79e-02	4.74e+00	6.77e-02	2.72e+00	6.81e-02
58	56.0901	32.1771	2.8	26	1,2	K7	16.42	14.92	12.49	11.28	10.62	5.32e+01	5.84e-01	4.80e+01	5.73e-01	4.16e+01	2.42e-01	3.53e+01	2.36e-01
59	56.0913	32.2032	14.0	—	3	M4	16.37	14.57	12.28	11.40	11.09	1.43e+01	2.09e-01	8.91e+00	1.13e-01	6.13e+00	6.78e-02	4.04e+00	1.10e-01
60	56.0929	32.0952	30.0	25	1	K8	15.88	14.45	12.55	11.28	10.70	2.76e+01	3.23e-01	2.34e+01	2.51e-01	2.06e+01	1.54e-01	2.83e+01	2.95e-01
61	56.0930	32.2002	8.4	—	3	M1	16.35	14.78	12.56	11.60	11.10	1.52e+01	2.96e-01	1.66e+01	1.93e-01	1.67e+01	1.41e-01	1.90e+01	2.11e-01
62	56.0941	32.0316	1.0	25	1	M2.5	16.01	14.40	12.12	11.15	10.79	1.35e+01	2.91e-01	1.10e+01	1.44e-01	8.44e+00	6.38e-02	6.76e+00	6.39e-02
63	56.0982	32.1594	1.7	—	3	M5	17.72	15.89	13.50	12.74	12.40	4.81e+00	5.23e-02	4.13e+00	3.72e-02	3.10e+00	4.29e-02	2.92e+00	7.73e-02
64	56.0986	32.1129	10.0	48	1,2,3,4	M2.5	15.83	14.27	12.23	11.38	11.07	1.30e+01	1.44e-01	8.89e+00	6.93e-02	6.19e+00	6.60e-02	3.27e+00	5.27e-02
65	56.1024	32.0659	4.9	57	1,3,4	M1	17.29	15.54	12.82	11.81	11.37	9.91e+00	1.41e-01	6.82e+00	7.41e-02	4.64e+00	7.81e-02	—	—
66	56.1065	32.1048	7.3	52	1,3	M2.25	17.85	15.98	12.98	11.70	11.14	1.55e+01	1.75e-01	1.25e+01	1.22e-01	9.82e+00	1.03e-01	1.05e+01	2.08e-01
67	56.1065	32.1919	5.4	24	1,2,3	M0	16.47	14.85	12.48	11.27	10.64	4.36e+01	7.81e-01	4.11e+01	7.02e-01	3.58e+01	3.29e-01	4.81e+01	3.75e-01
68	56.1066	32.2083	8.4	63	1,2,4	M0.5	14.79	13.59	11.82	10.95	10.68	1.68e+01	2.56e-01	1.11e+01	1.34e-01	7.55e+00	7.55e-02	4.49e+00	6.18e-02
69	56.1110	32.0662	3.1	30	1,2,3,4	M4.75	16.20	14.33	11.80	10.94	10.59	1.93e+01	2.23e-01	1.26e+01	1.49e-01	8.79e+00	8.03e-02	5.22e+00	1.33e-01
70	56.1112	32.1390	8.9	29	1	M0.5	17.72	16.03	12.99	11.56	10.84	3.12e+01	4.26e-01	2.76e+01	3.01e-01	1.99e+01	1.94e-01	1.95e+01	2.54e-01
71	56.1126	32.0788	9.1	—	3	M1	15.07	13.77	11.95	11.14	10.85	1.44e+01	1.80e-01	9.96e+00	1.49e-01	6.82e+00	7.61e-02	3.88e+00	1.06e-01
72	56.1137	32.1216	1.5	—	3	M4.75	18.57	16.81	14.43	13.59	13.27	2.03e+00	2.77e-02	1.39e+00	1.76e-02	9.29e-01	2.54e-02	7.75e-01	5.00e-02
73	56.1153	32.5638	2.6	31	1	—	15.87	14.34	12.10	11.23	10.87	—	—	—	—	—	—	—	—
74	56.1162	32.1255	5.4	23	1,2,4	M2	15.80	14.23	12.13	11.27	10.97	1.40e+01	2.01e-01	9.78e+00	9.15e-02	6.30e+00	9.11e-02	3.39e+00	8.18e-02
75	56.1172	32.2667	2.7	52	1	M3.25	15.98	14.38	12.21	11.35	11.02	1.29e+01	1.97e-01	8.79e+00	1.10e-01	6.35e+00	7.15e-02	3.71e+00	8.04e-02
76	56.1186	32.1229	7.0	52	1,2,3,4	K6.5	14.44	13.30	11.67	10.85	10.58	1.65e+01	2.50e-01	1.12e+01	1.14e-01	7.29e+00	1.16e-01	4.04e+00	1.01e-01
77	56.1309	32.1915	1.4	—	3	M5.25	18.27	16.15	13.48	12.74	12.34	4.68e+00	7.17e-02	3.60e+00	7.48e-02	2.22e+00	9.20e-02	1.49e+00	1.70e-01
78	56.1314	32.1458	10.8	—	3,4	K2	—	—	10.69	9.97	9.72	3.89e+01	6.15e-01	2.66e+01	2.96e-01	1.80e+01	1.46e-01	1.05e+01	2.07e-01
79	56.1349	32.0576	1.6	—	3	M5.5	20.68	18.09	14.88	14.04	13.48	2.37e+00	2.96e-02	2.05e+00	2.29e-02	1.63e+00	6.07e-02	—	—
80	56.1357	32.1488	6.7	—	3	M3	16.05	14.43	12.11	11.13	10.76	1.77e+01	2.94e-01	1.40e+01	1.39e-01	1.09e+01	1.30e-01	9.29e+00	1.65e-01
81	56.1364	32.1437	2.6	—	3,4	G6	—	—	10.28	9.65	9.43	4.86e+01	6.93e-01	3.47e+01	2.77e-01	2.25e+01	2.15e-01	1.26e+01	2.76e-01
82	56.1365	32.1544	5.5	33	1,4	M3.25	16.14	14.68	12.35	11.37	11.01	1.39e+01	1.80e-01	1.00e+01	1.22e-01	7.12e+00	8.31e-02	4.88e+00	1.40e-01
83	56.1367	32.0704	5.3	23	1	M5	18.61	16.49	13.74	12.90	12.52	4.15e+00	5.86e-02	2.86e+00	4.19e-02	1.90e+00	5.41e-02	—	—
84	56.1388	32.1610	2.2	25	1	M2	15.10	13.99	12.33	11.37	11.06	2.13e+01	3.10e-01	1.62e+01	2.98e-01	1.20e+01	1.46e-01	7.49e+00	1.75e-01
85	56.1408	31.9751	3.9	27	1	—	18.13	16.23	13.49	12.27	11.61	1.13e+01	1.95e-01	9.15e+00	9.60e-02	6.87e+00	8.20e-02	6.63e+00	5.42e-02
86	56.1416	32.1484	16.4	—	2,4	M0	—	—	11.85	10.98	10.70	1.58e+01	2.32e-01	1.06e+01	1.18e-01	7.62e+00	1.00e-01	5.25e+00	1.65e-01
87	56.1419	32.1159	3.4	—	3	M7.25	19.47	17.26	—	—	—	4.67e+00	6.25e-02	4.28e+00	4.42e-02	4.28e+00	6.56e-02	4.86e+00	1.10e-01
88	56.1450	31.9487	3.5	35	1	—	16.82	15.17	13.03	12.09	11.62	1.26e+01	1.21e-01	8.60e+00	1.18e-01	6.43e+00	6.74e-02	5.19e+00	1.12e-01
89	56.1453	32.1094	5.4	—	2,3,4	K5.5	14.55	13.35	11.51	10.61	10.31	2.32e+01	3.68e-01	1.63e+01	1.91e-01	1.13e+01	1.30e-01	6.64e+00	1.27e-01
90	56.1459	32.1493	1.8	—	3	M4.75	18.08	16.63	14.87	14.11	13.71	1.79e+00	4.59e-02	1.32e+00	3.15e-02	1.01e+00	1.04e-01	5.88e-01	2.12e-01
91	56.1460	32.1270	4.5	42	1,2	K6.5	14.22	15.14	10.99	10.07	9.76	4.18e+01	6.16e-01	2.80e+01	3.81e-01	1.81e+01	1.49e-01	1.17e+01	1.38e-01
92	56.1477	32.1490	1.9	—	3	M5.25	17.71	16.05	13.25	12.31	11.83	9.19e+00	1.78e-01	8.21e+00	1.22e-01	7.54e+00	1.48e-01	7.48e+00	1.86e-01
93	56.1480	32.1346	1.7	—	3	M5.25	18.26	16.39	13.64	12.72	12.33	4.72e+00	7.17e-02	3.38e+00	4.57e-02	2.35e+00	3.62e-02	1.14e+00	9.20e-02
94	56.1487	32.0510	12.0	34	1	M3.25	19.06	17.36	14.13	12.78	11.84	1.15e+01	1.96e-01	1.18e+01	1.63e-01	1.16e+01	9.46e-02	1.30e+01	1.35e-01
95	56.1539	32.1126	1.7	—	2,4	G3	—	—	9.21	8.48	8.19	1.85e+02	3.63e+00	1.03e+02	2.98e+00	1.15e+02	7.00e-01	8.48e+01	6.24e-01
96	56.1541	32.1429	2.5	—	3	M4.75	17.53	15.73	13.06	12.07	11.59	1.05e+01	1.62e-01	8.46e+00	1.08e-01	6.92e+00	1.27e-01	6.27e+00	1.59e-01
97	56.1558	32.1033	6.2	—	2,4	K7	15.17	13.88	12.08	11.14	10.87	1.41e+01	2.05e-01	9.42e+00	1.10e-01	6.86e+00	8.12e-02	3.96e+00	1.28e-01
98	56.1558	32.2067	19.8	31	1,3	M2	17.89	16.02	13.07	11.84	11.28	1.32e+01	2.18e-01	1.15e+01	1.27e-01	8.93e+00	1.04e-01	1.15e+01	2.06e-01
99	56.1559	32.1502	8.4	38	1,4	M1	16.28	14.91	12.48	11.44	10.99	2.25e+01	4.00e-01	2.04e+01	3.67e-01	1.89e+01	2.91e-01	2.39e+01	3.96e-01
100	56.1574	32.2050	3.3	58	1,3,4	M4.5	17.69	15.68	13.04	12.15	11.79	8.40e+00	8.81e-02	5.95e+00	5.99e-02	4.12e+00	5.34e-02	1.97e+00	4.63e-02

Table 1—Continued

ID	Ra	Dec	P	PS	$Ref_P$	SpT	$R_C$	$I_C$	J	H	$K_S$	[3.6]	[3.6] error	[4.5]	[4.5] error	[5.8]	[5.8] error	[8.0]	[8.0] error
	(deg)	(deg)	(days)	<sup>1</sup>	<sup>2</sup>		<sup>3</sup>		(mag)						(mJy)				
101	56.1578	32.1345	8.2	30	1,3	K7	15.58	14.12	11.69	10.48	9.83	6.03e+01	1.51e+00	6.55e+01	8.83e-01	5.62e+01	4.69e-01	5.83e+01	5.54e-01
102	56.1583	32.0582	8.6	33	1,2	K6	14.66	13.35	11.45	10.44	9.87	6.15e+01	6.67e-01	4.52e+01	8.42e-01	4.40e+01	3.47e-01	5.27e+01	4.02e-01
103	56.1599	32.2166	13.5	—	4	M0	15.97	14.64	12.81	11.93	11.65	7.73e+00	1.08e-01	4.99e+00	4.89e-02	3.22e+00	4.41e-02	1.52e+00	6.94e-02
104	56.1602	32.1266	5.1	45	1,2,3,4	K6	14.52	13.21	11.18	10.23	9.85	3.77e+01	8.08e-01	3.67e+01	4.80e-01	3.81e+01	2.85e-01	5.69e+01	5.22e-01
105	56.1606	32.1335	7.3	29	1,2,3,4	M1.25	15.85	14.32	11.94	10.90	10.47	2.74e+01	4.85e-01	2.45e+01	2.55e-01	1.88e+01	2.27e-01	2.65e+01	3.43e-01
106	56.1612	32.1491	2.1	—	3	M3.25	15.99	14.45	12.45	11.57	11.28	1.18e+01	1.61e-01	7.93e+00	8.67e-02	5.09e+00	1.39e-01	3.13e+00	1.50e-01
107	56.1613	32.1450	2.4	31	1,3,4	K3	15.60	14.01	11.19	9.97	9.49	5.52e+01	9.19e-01	4.12e+01	3.49e-01	2.72e+01	2.71e-01	1.50e+01	2.52e-01
108	56.1616	32.3182	4.8	56	1	—	17.16	15.47	13.34	12.47	12.14	5.25e+00	8.46e-02	3.49e+00	5.26e-02	2.62e+00	7.57e-02	1.79e+00	1.08e-01
109	56.1632	32.1551	1.6	—	2,3,4	G8	—	—	10.07	9.14	8.77	9.01e+01	2.24e+00	7.49e+01	9.51e-01	5.02e+01	5.20e-01	2.87e+01	6.57e-01
110	56.1633	32.1625	3.9	52	1,3,4	M2	16.30	14.77	12.46	11.46	11.09	1.66e+01	2.69e-01	1.48e+01	1.71e-01	1.27e+01	1.47e-01	1.41e+01	3.25e-01
111	56.1643	32.1689	1.5	—	3	M5	17.60	16.06	13.85	13.10	12.72	3.16e+00	4.50e-02	2.33e+00	3.03e-02	1.37e+00	4.53e-02	1.28e+00	1.37e-01
112	56.1638	32.6037	0.2	24	1	—	19.75	18.64	16.28	15.33	15.12	—	—	—	—	—	—	—	—
113	56.1658	32.3012	9.5	38	1	M3.75	16.85	15.00	12.23	11.28	10.78	2.21e+01	3.09e-01	1.75e+01	2.43e-01	1.37e+01	1.10e-01	1.35e+01	1.05e-01
114	56.1692	32.3864	4.1	45	1	—	—	—	12.80	11.83	11.55	8.07e+00	1.24e-01	5.61e+00	5.73e-02	3.69e+00	4.76e-02	2.16e+00	3.49e-02
115	56.1721	32.1737	3.7	—	3	M4.75	16.05	14.76	12.56	11.77	11.44	9.64e+00	1.52e-01	7.34e+00	7.02e-02	4.75e+00	7.29e-02	1.86e+00	7.88e-02
116	56.1721	32.0815	1.6	—	3	M5	—	—	14.51	13.71	13.28	1.95e+00	2.96e-02	1.43e+00	1.77e-02	8.46e-01	3.85e-02	—	—
117	56.1732	32.1776	1.7	—	3	M5.75	19.07	18.16	15.46	14.86	14.25	1.02e+00	1.70e-02	7.93e-01	1.10e-02	5.05e-01	4.12e-02	3.60e-01	2.61e-02
118	56.1739	32.2006	2.1	28	1	M5	18.68	16.09	13.26	12.02	11.42	1.12e+01	1.16e-01	8.13e+00	7.94e-02	6.70e+00	7.23e-02	6.61e+00	1.46e-01
119	56.1753	32.1503	16.0	38	1	—	16.27	14.21	11.79	10.67	10.13	2.47e+01	3.83e-01	2.21e+01	4.64e-01	2.61e+01	4.01e-01	2.10e+01	3.84e-01
120	56.1774	32.1674	3.6	—	3	M4.25	19.18	17.11	13.63	12.36	11.79	1.18e+01	1.33e-01	1.12e+01	1.02e-01	9.82e+00	9.29e-02	1.02e+01	1.64e-01
121	56.1776	32.1054	12.0	25	1,2,3,4	M1	15.10	13.95	12.52	11.77	11.54	8.41e+00	1.09e-01	5.26e+00	5.70e-02	3.51e+00	8.74e-02	2.64e+00	1.48e-01
122	56.1791	32.0259	1.0	24	1	—	—	—	15.22	14.66	11.74	—	—	—	—	—	4.39e-01	—	—
123	56.1824	32.1751	10.6	26	1,2	M1.25	15.92	14.40	12.29	11.25	10.83	1.82e+01	2.31e-01	1.85e+01	1.77e-01	2.08e+01	1.29e-01	3.27e+01	2.58e-01
124	56.1843	32.1465	1.8	—	3	M5.75	19.20	17.42	14.59	13.71	13.34	2.21e+00	2.77e-02	1.49e+00	1.78e-02	5.70e-01	4.44e-02	—	8.85e-02
125	56.1845	32.1769	1.5	—	3	M5.25	20.34	18.00	15.38	14.75	14.37	8.78e-01	1.18e-02	6.42e-01	1.35e-02	3.74e-01	3.87e-02	—	6.35e-02
126	56.1902	32.1863	1.3	—	3	M4.75	19.33	17.46	15.10	14.29	13.95	1.14e+00	2.28e-02	8.23e-01	1.39e-02	5.11e-01	4.84e-02	3.04e-01	1.36e-01
127	56.2034	32.2227	6.9	61	1	M2.75	16.80	15.20	13.10	12.24	11.94	5.62e+00	7.73e-02	3.86e+00	3.98e-02	2.63e+00	5.02e-02	1.57e+00	7.50e-02
128	56.2123	32.2693	13.1	45	1	M3.25	16.29	14.60	12.33	11.49	11.13	1.27e+01	1.62e-01	8.85e+00	7.72e-02	6.04e+00	6.75e-02	3.65e+00	1.13e-01
129	56.2240	32.1144	9.6	22	1	M4	18.04	16.03	13.33	12.37	11.96	6.04e+00	9.19e-02	4.42e+00	5.30e-02	3.16e+00	4.39e-02	1.52e+00	3.05e-02
130	56.2317	32.1555	3.1	60	1	K4	16.02	14.39	11.85	10.75	10.36	2.41e+01	3.83e-01	1.77e+01	1.75e-01	1.16e+01	9.29e-02	6.66e+00	9.29e-02
131	56.2338	32.0990	3.3	33	1	M2.75	16.50	14.95	13.07	12.27	11.99	5.57e+00	6.23e-02	3.54e+00	4.91e-02	2.54e+00	2.89e-02	1.42e+00	3.62e-02
132	56.2339	32.1542	2.5	29	1	K0	14.69	5.26	11.02	9.99	9.47	6.62e+01	1.06e+00	6.28e+01	9.42e-01	4.42e+01	3.45e-01	3.81e+01	2.56e-01
133	56.2563	32.1809	1.9	51	1,2	K0	14.26	13.26	11.86	11.13	10.88	1.36e+01	2.08e-01	9.33e+00	9.06e-02	6.29e+00	5.62e-02	3.77e+00	7.11e-02
134	56.2573	32.2410	16.4	55	1,2	K4	14.80	13.46	11.34	10.40	10.04	3.18e+01	4.26e-01	1.91e+01	2.68e-01	1.45e+01	9.37e-02	8.61e+00	6.94e-02
135	56.3166	32.5144	4.1	44	1	—	15.17	13.90	11.96	11.07	10.77	1.59e+01	1.28e-01	1.05e+01	7.09e-02	7.04e+00	6.04e-02	3.78e+00	4.31e-02
136	56.3250	32.3258	7.9	37	1	—	17.72	15.87	13.35	12.40	12.05	6.12e+00	6.11e-02	3.96e+00	5.11e-02	2.55e+00	3.59e-02	1.49e+00	3.48e-02
137	56.3353	32.1096	6.9	41	1	M1	14.90	13.42	11.12	9.98	9.35	7.93e+01	1.82e+00	8.07e+01	1.36e+00	7.68e+01	5.40e-01	7.31e+01	6.16e-01
138	56.3371	32.3034	5.0	28	1	—	18.43	16.67	15.59	14.70	14.46	5.55e-01	1.27e-02	3.86e-01	8.06e-03	2.38e-01	3.39e-02	1.65e-01	2.51e-02
139	56.3378	32.3049	5.0	58	1	—	17.70	15.72	12.87	11.82	11.40	1.17e+01	1.78e-01	7.51e+00	7.42e-02	5.26e+00	7.26e-02	2.81e+00	2.78e-02
140	56.3846	32.0542	0.7	31	1	M3	16.03	14.60	12.89	12.14	11.89	5.40e+00	8.36e-02	3.88e+00	4.46e-02	2.58e+00	3.46e-02	1.48e+00	2.55e-02
141	56.3980	31.9405	9.6	49	1	—	16.64	15.08	12.76	11.79	11.41	9.91e+00	1.95e-01	6.12e+00	1.74e-01	3.87e+00	7.50e-02	2.16e+00	4.20e-02
142	56.4327	32.4098	14.3	50	1	—	17.62	15.82	13.42	12.53	12.17	4.97e+00	4.36e-02	3.34e+00	3.24e-02	2.36e+00	2.40e-02	1.37e+00	2.43e-02
143	56.4448	32.4802	10.5	33	1	—	—	—	12.77	11.79	11.41	8.56e+00	8.15e-02	6.04e+00	5.06e-02	4.62e+00	8.24e-02	2.49e+00	3.74e-02

<sup>1</sup>Power spectrum peak<sup>2</sup>Rotation period reported in this paper (1), Koziloglu et al. (2005) (2), Littlefair et al. (2005) (3), and Cohen et al. (2004) (4)<sup>3</sup>The  $R_C$  and  $I_C$  photometry of the following stars have been taken from Cohen et al. (2004), ID=45,49,79,82,87,96,111

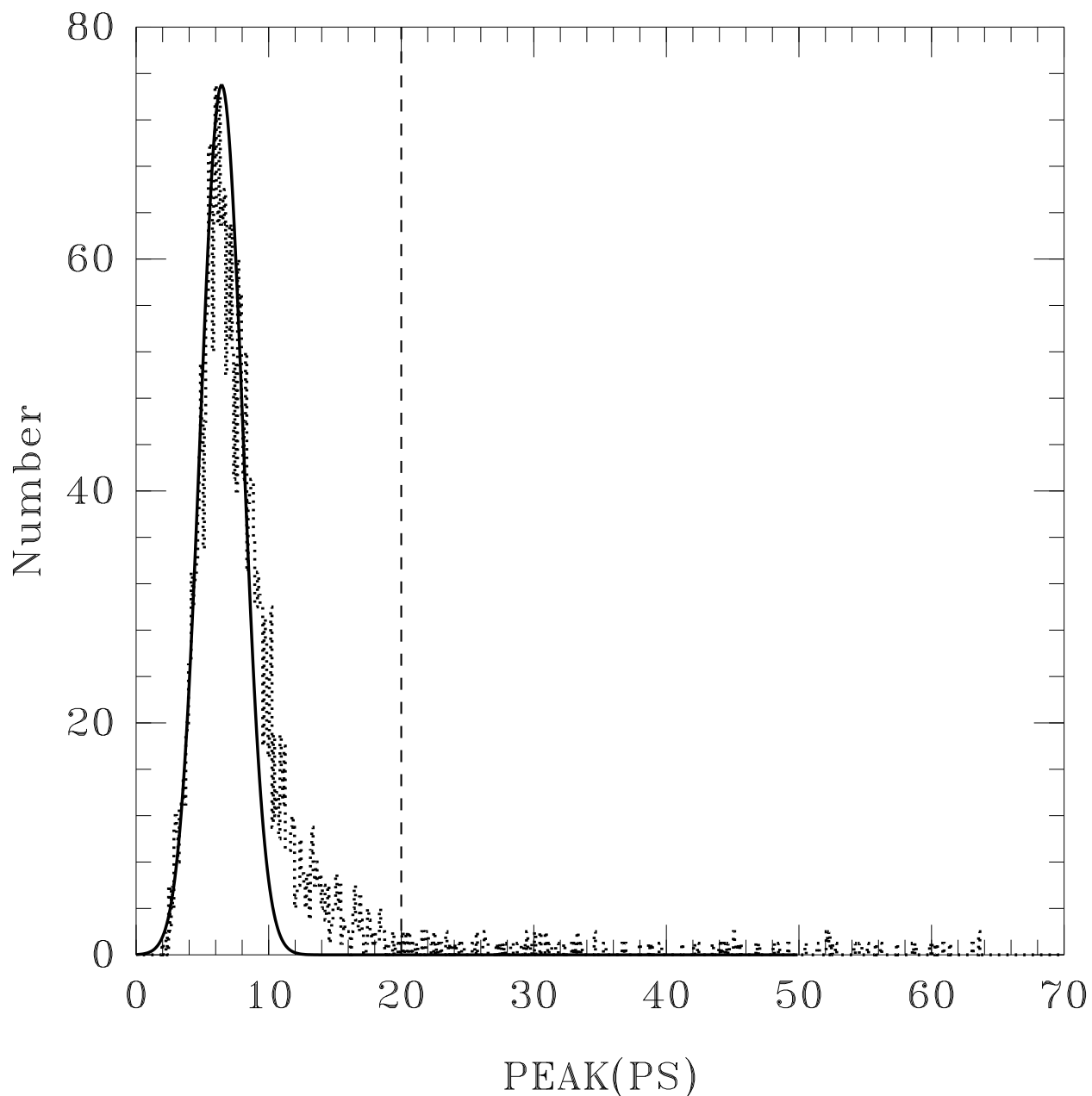


Fig. 1.— This is a plot of the distribution of power spectrum peaks for the entire sample of stars in the IC 348 data set. The dotted line is a histogram of the maximum power spectrum peak of each star, and the solid line is a Gaussian fit to the left side of the distribution of power spectrum peaks. Non-white noise is likely to raise a particular peak above what white noise alone would provide. Such systematic noise creates the shoulder above the Gaussian curve on the right wing of the distribution of peaks. This additional non-white noise makes period determinations for stars with power spectrum peaks lower than  $\sim 20$  unreliable.

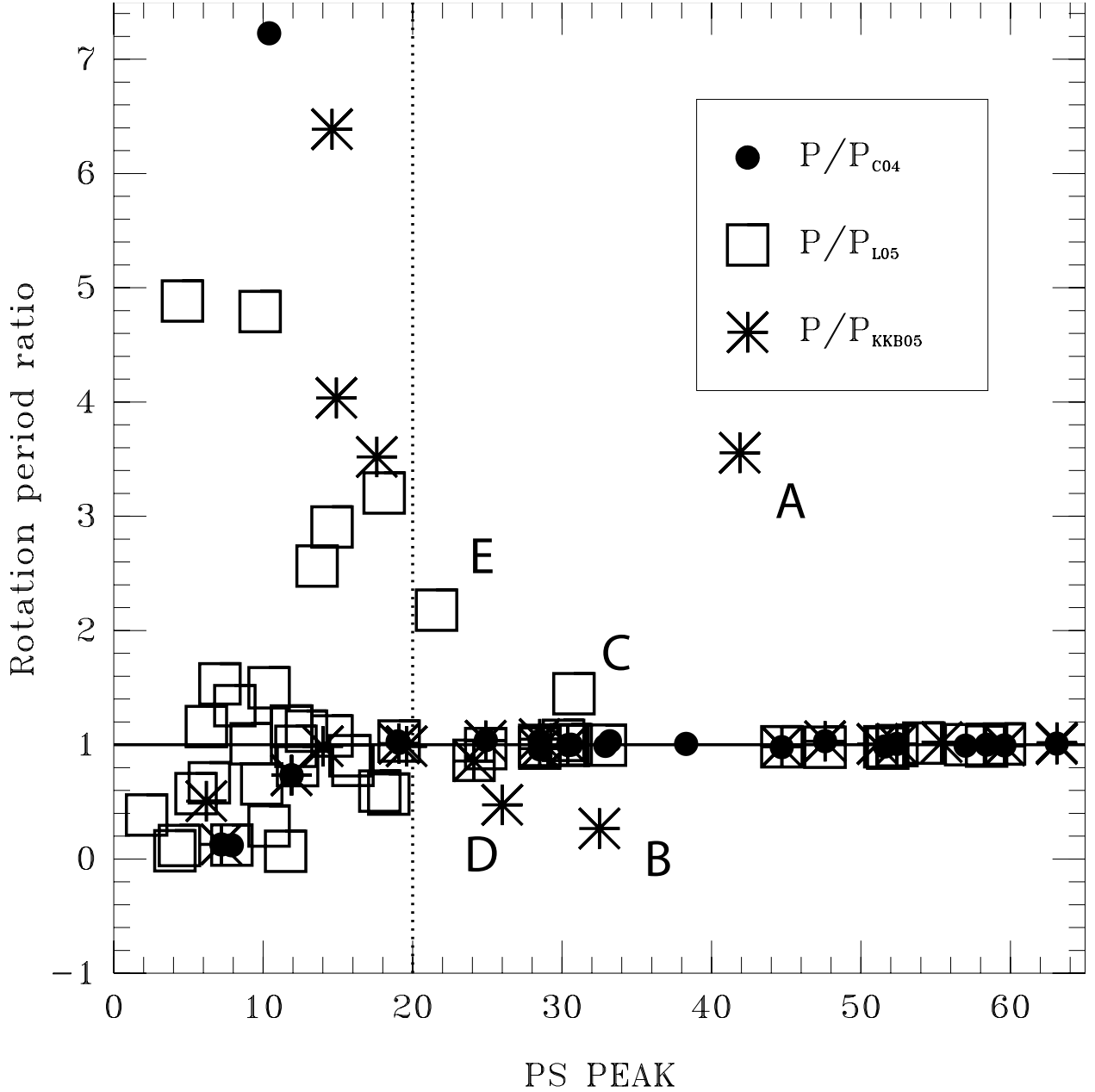


Fig. 2.— This is a plot of the ratio of our rotation periods to those from Cohen et al. (2004, C04), Littlefair et al. (2005, L05), and Kızıloğlu et al. (2005, KKB05) as a function of power spectrum peak from our light curves. The values start to diverge for power spectra peaks lower than  $\sim 20$ . Based on the peak distribution from Figure 1 and these ratios, we adopt a power spectrum peak of 22.0 as the threshold above which we consider the measured periodic signal to be an accurate representation of the stellar rotation period. The disagreement with rotation periods from the literature for stars A through E is discussed in the text and in Figure 3.

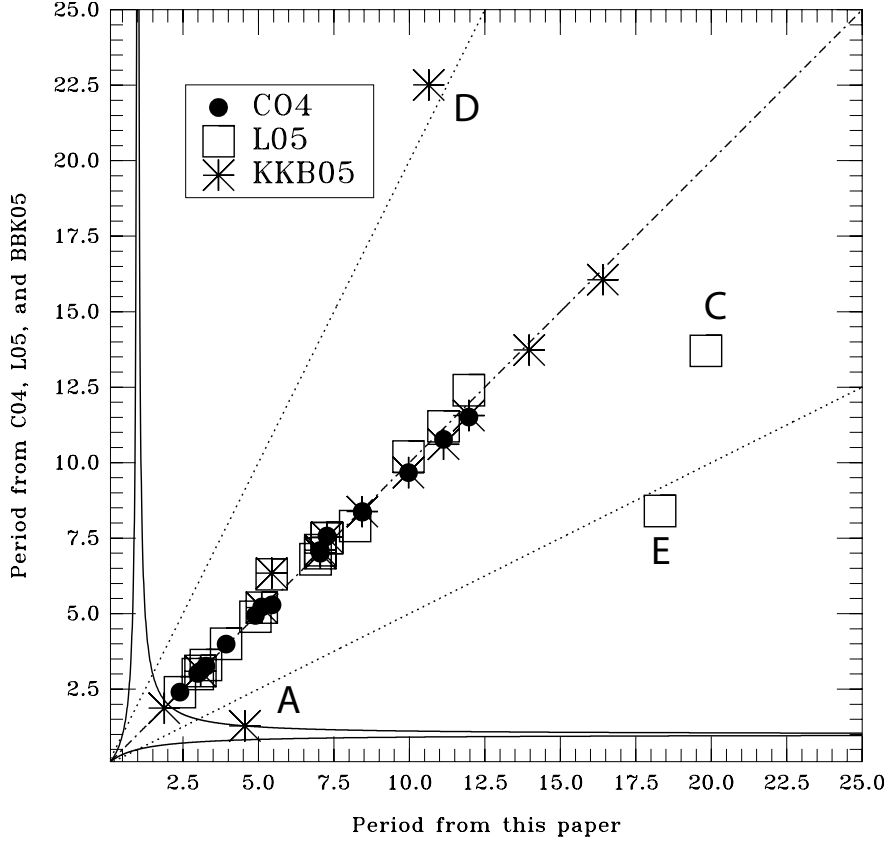


Fig. 3.— This figure is another comparison of our IC 348 periods to those obtained by other groups. Only five stars for which we measure power spectra peaks above 20 show significant discrepancies between our periods and those from the literature. For star A, Kızıloğlu et al. (2005, KKB05) find a period of 1.28 days, where we measure a period of 4.55 days. Their shorter period is a result of the beating of our period at a 1-day sampling interval, of the form  $1/P_{\text{beating}} = \pm 1 \pm (1/P)$  (plotted as a solid line). For object B and D, we find shorter periods than those found by KKB05; their periods are likely harmonics of the real periods (the two dotted lines represent factor-of-two harmonics). Our period for object C, 19.8 days, shows a discrepancy with the 13.4-day period found by Littlefair et al. (2005, L05) which cannot easily be explained. Longer periods have greater uncertainty, however, and since our observational baseline is twice as long as that of L05 (52 *versus* 26 days), we take our period to be closer to the correct value. Our period for object E is 18.3 days while L05 measured a period of 8.4 days. In this case, our period is likely a harmonic of the real period.



# IC 348, ALL STARS

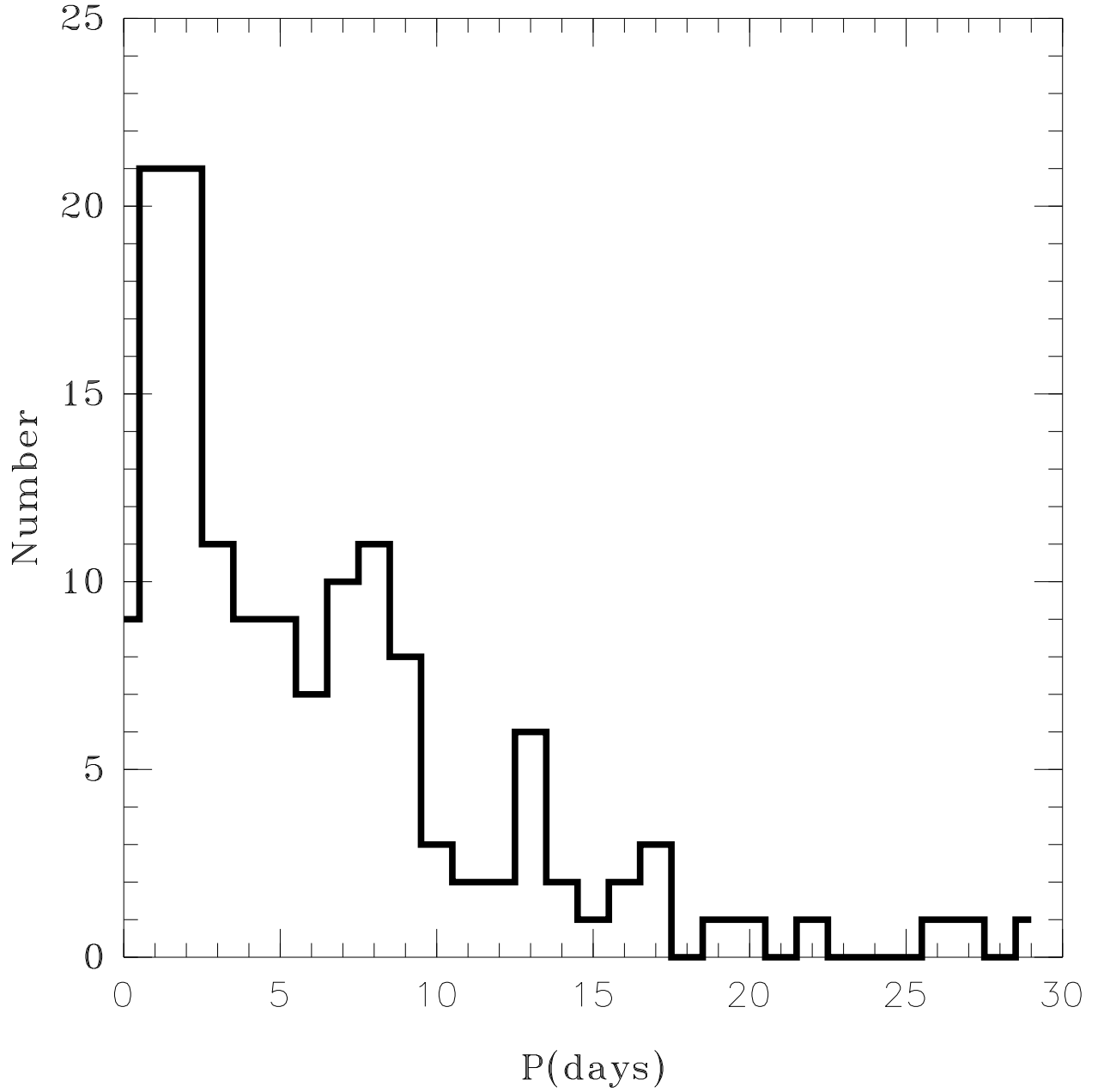


Fig. 4.— A histogram of all 143 know rotation periods in IC 348 from our data and the literature.

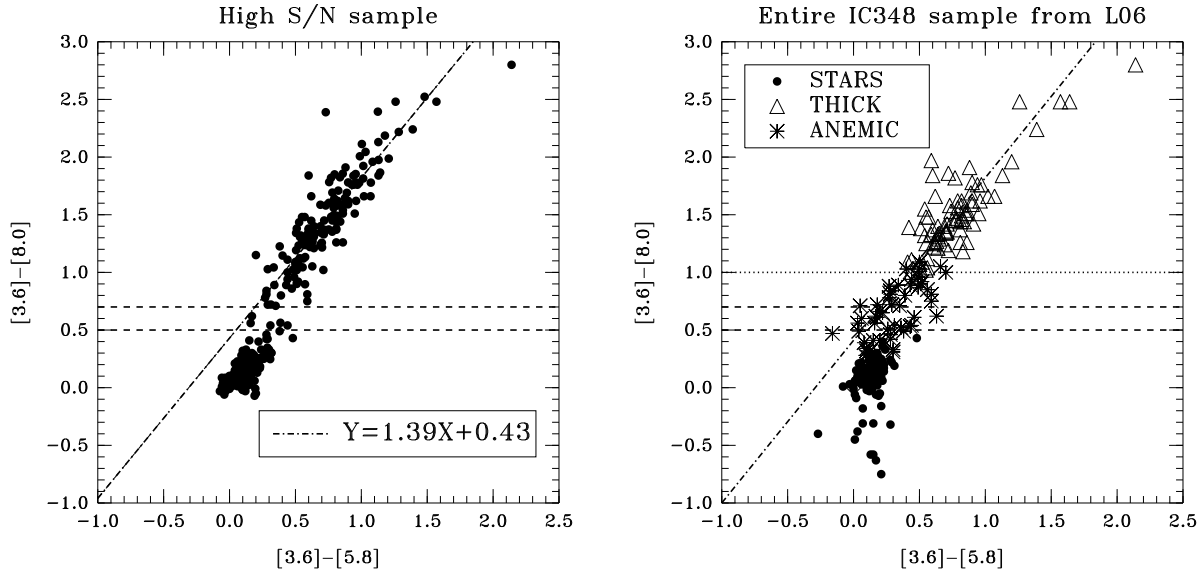


Fig. 5.— The plot on the left shows the  $[3.6]-[8.0]$  vs.  $[3.6]-[5.8]$  colors of 435 PMS stars collected from the literature with photometric errors less than 0.1 mag. Objects with  $[3.6]-[8.0] > 0.7$  are stars with significant IR excess indicating the presence of a disk. Objects with  $[3.6]-[8.0] < 0.5$  are consistent with stellar photospheres. Only  $\sim 1\%$  of the stars have  $0.7 > [3.6]-[8.0] > 0.5$ . The dash-dotted line is a linear fit to the stars with disks. The plot on the right shows the entire sample of IC 348 members studied by Lada et al. (2006, L06 in this figure). Some of the objects classified as “anemic disks” by L06 seem to be photospheres of late type stars. The dotted line correspond to the disk identification criteria adopted by Rebull et al. (2006).

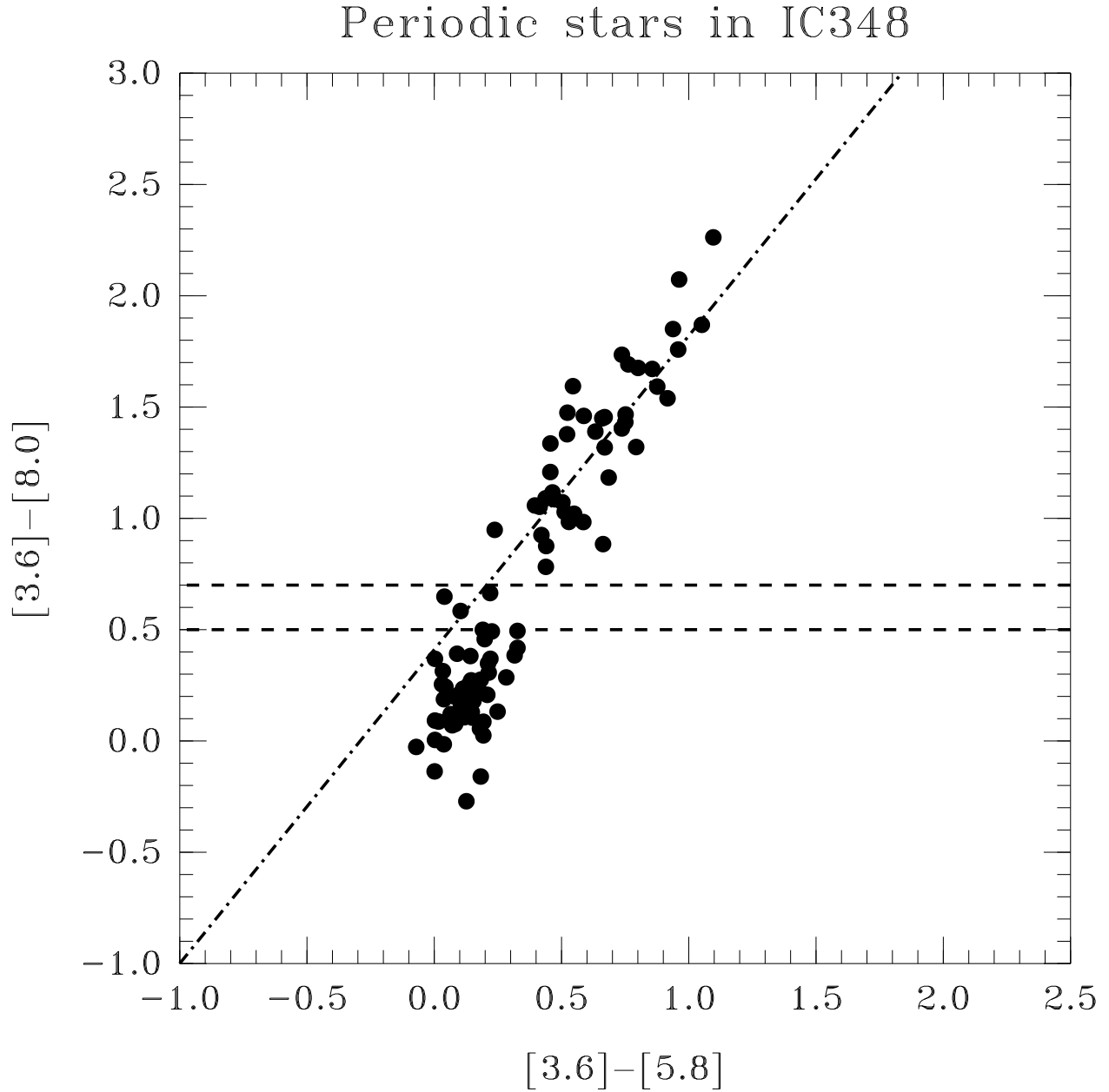


Fig. 6.— The  $[3.6]-[8.0]$  vs.  $[3.6]-[5.8]$  colors of the periodic stars in IC348. Stars with  $[3.6]-[3.8]$  colors  $> 0.7$  possess disks while stars with  $[3.6]-[3.8]$  colors  $< 0.5$  are diskless. Only three objects show a somewhat ambiguous disk identification.

IC 348, ALL SPTs

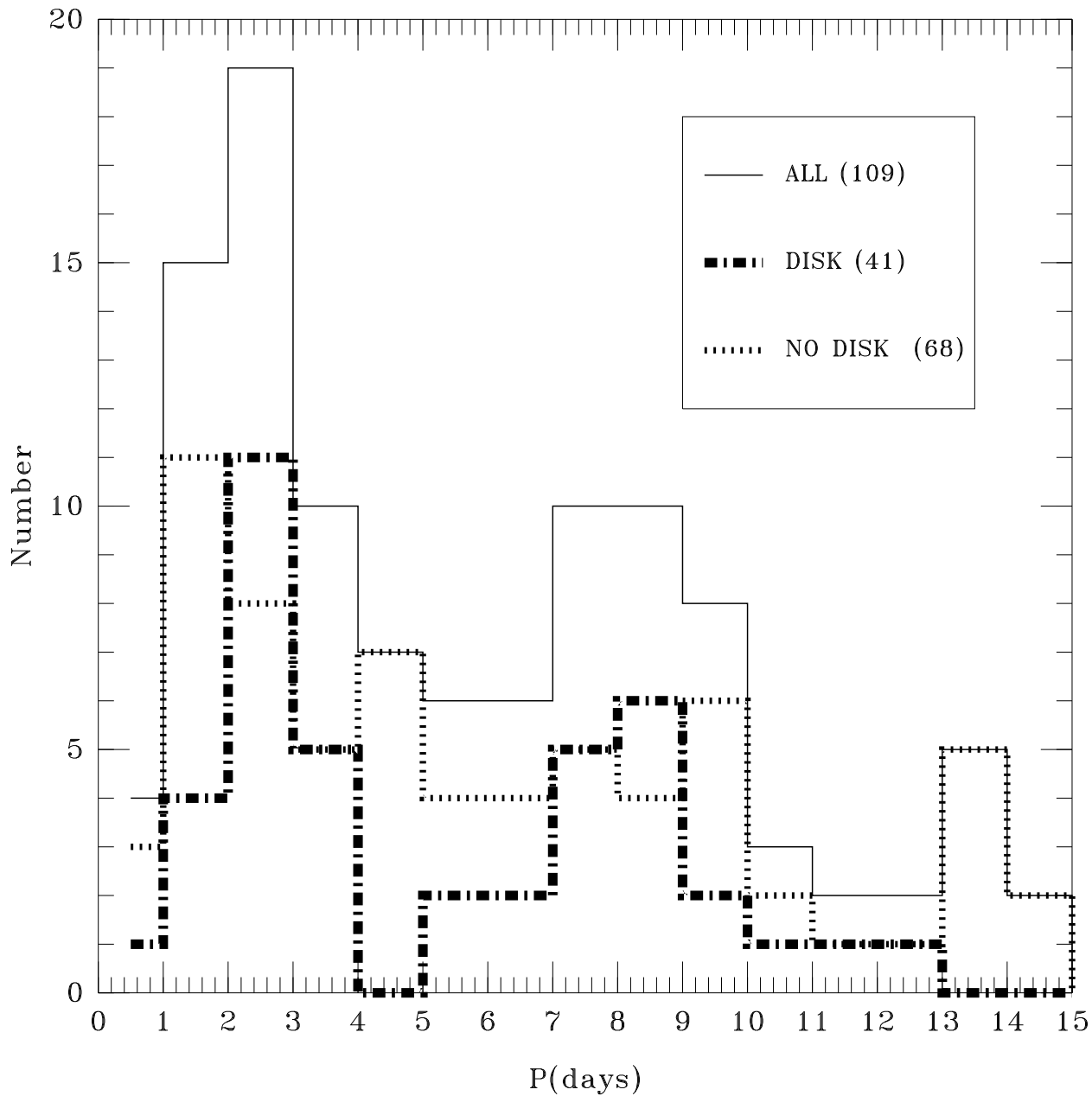


Fig. 7.— Period histogram for 109 IC 348 stars with rotation periods  $< 15$  days and  $[3.6] - [8.0]$  data. The three different lines represent all stars (solid), stars with an IR excess indicating the presence of a disk (dot-dash line), and stars with no detected disk signature (dotted line). A very clear bimodal distribution is seen for stars with disks; there is no clear correlation between the presence of a disk and the rotation period for the stars in IC 348.

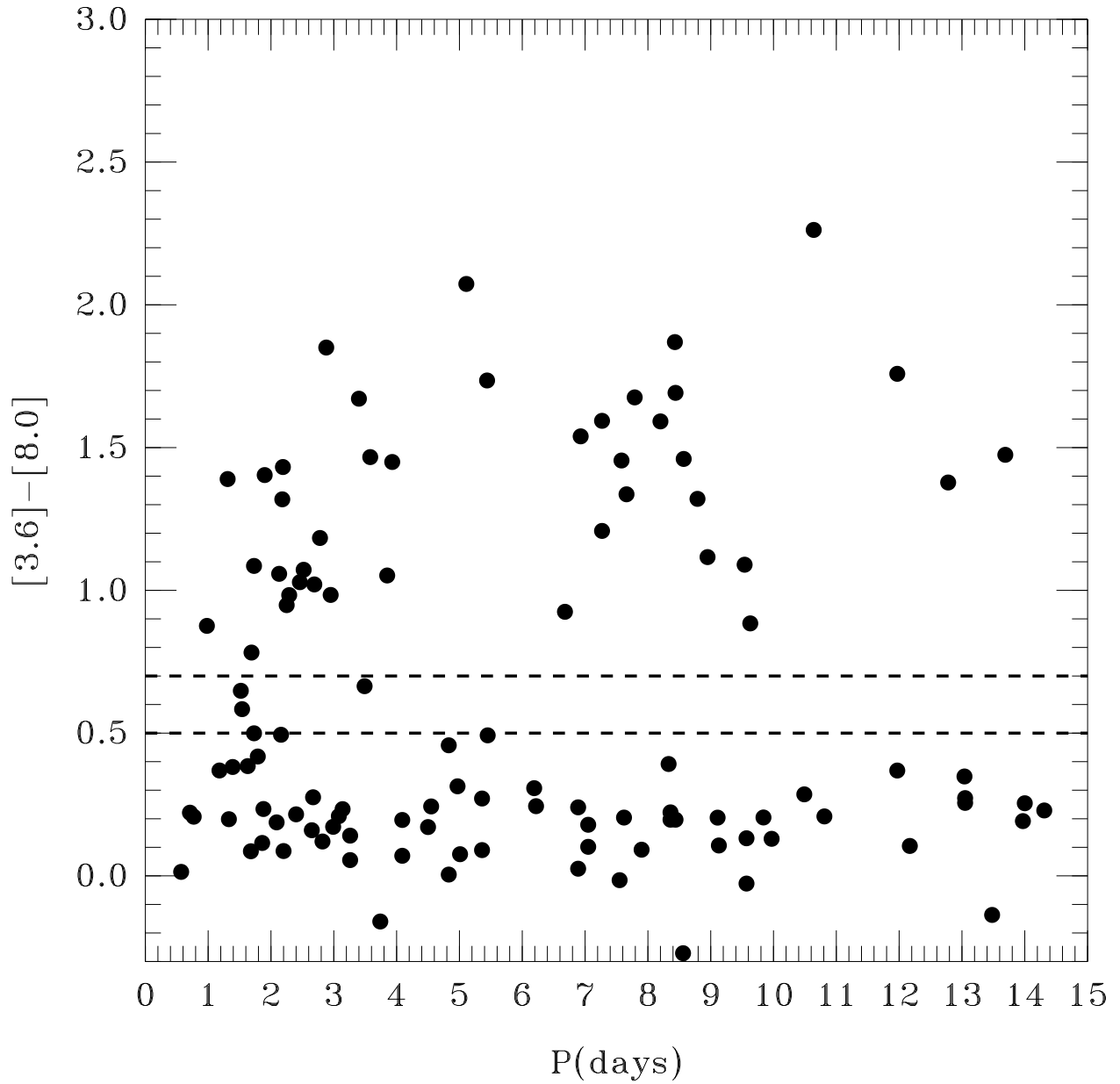


Fig. 8.— A plot of  $[3.6]-[8.0]$  color vs. period. We find no evidence for a correlation between period and the presence of an IR excess or the magnitude of the excess. A standard Spearman test yields over a 84% chance that the quantities are completely uncorrelated.

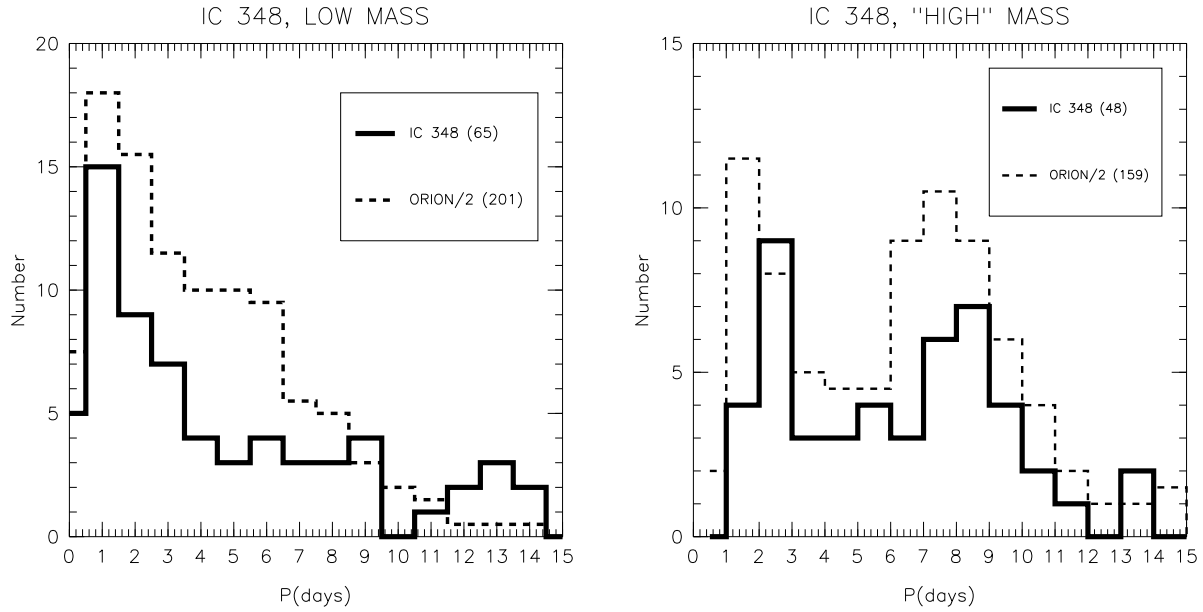


Fig. 9.— Period histograms for low and high mass stars in the IC 348 cluster with *Spitzer* data. The period distributions resemble those seen in the heart of the Orion Nebula Cluster (ONC) by H02, which are shown for comparison scaled down by a factor of two. Stars estimated to be less massive than  $0.25 M_{\odot}$  show a unimodal distribution dominated by fast rotators ( $P \sim 1\text{--}2$  days), while stars estimated to be more massive than  $0.25 M_{\odot}$  show a bimodal distribution with peaks at  $\sim 2$  and  $\sim 8$  days.

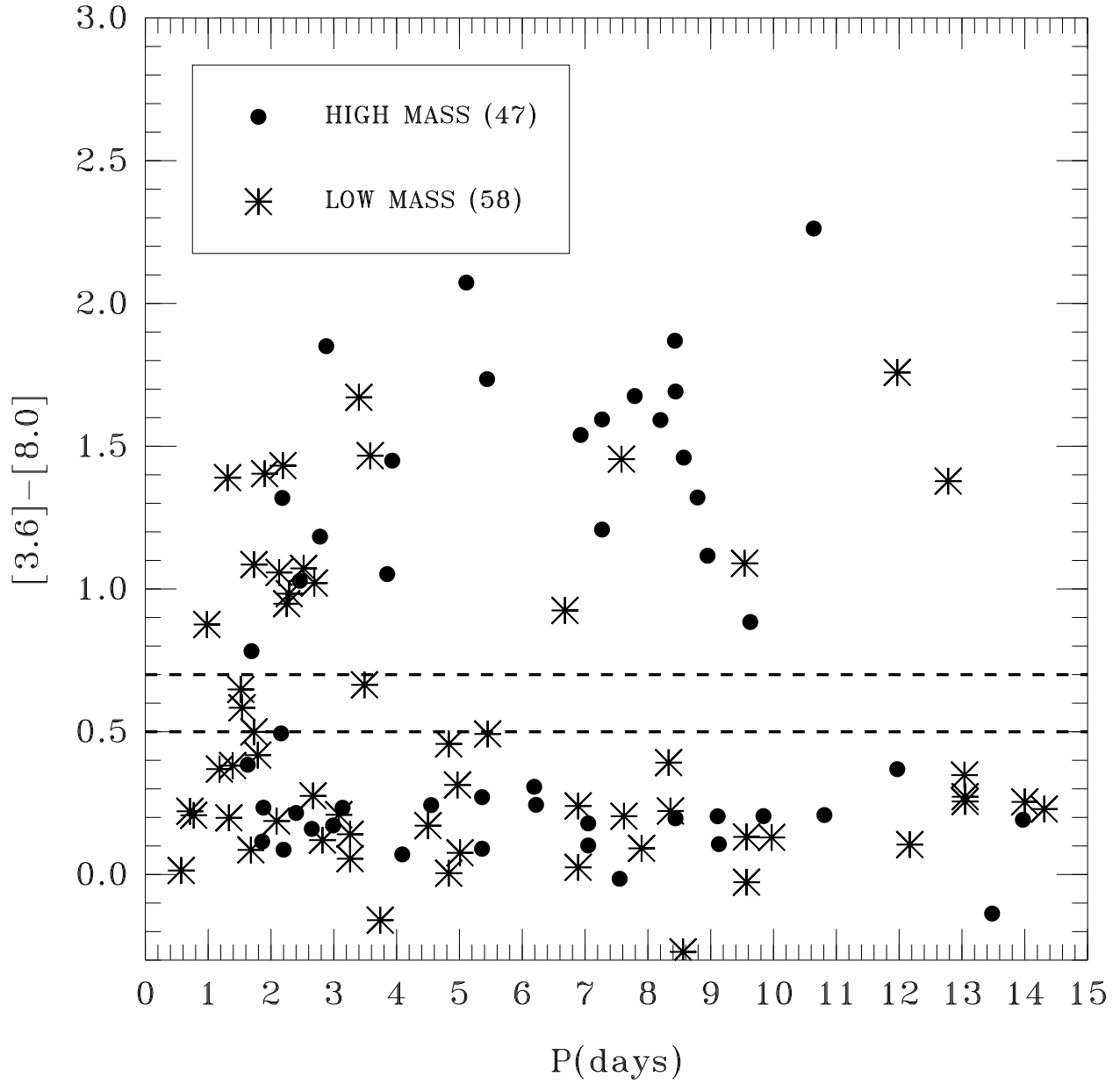


Fig. 10.—  $[3.6] - [8.0]$  color *vs.* period for low- and high-mass stars. There is no significant correlation between IR excess and the period of either type of star.

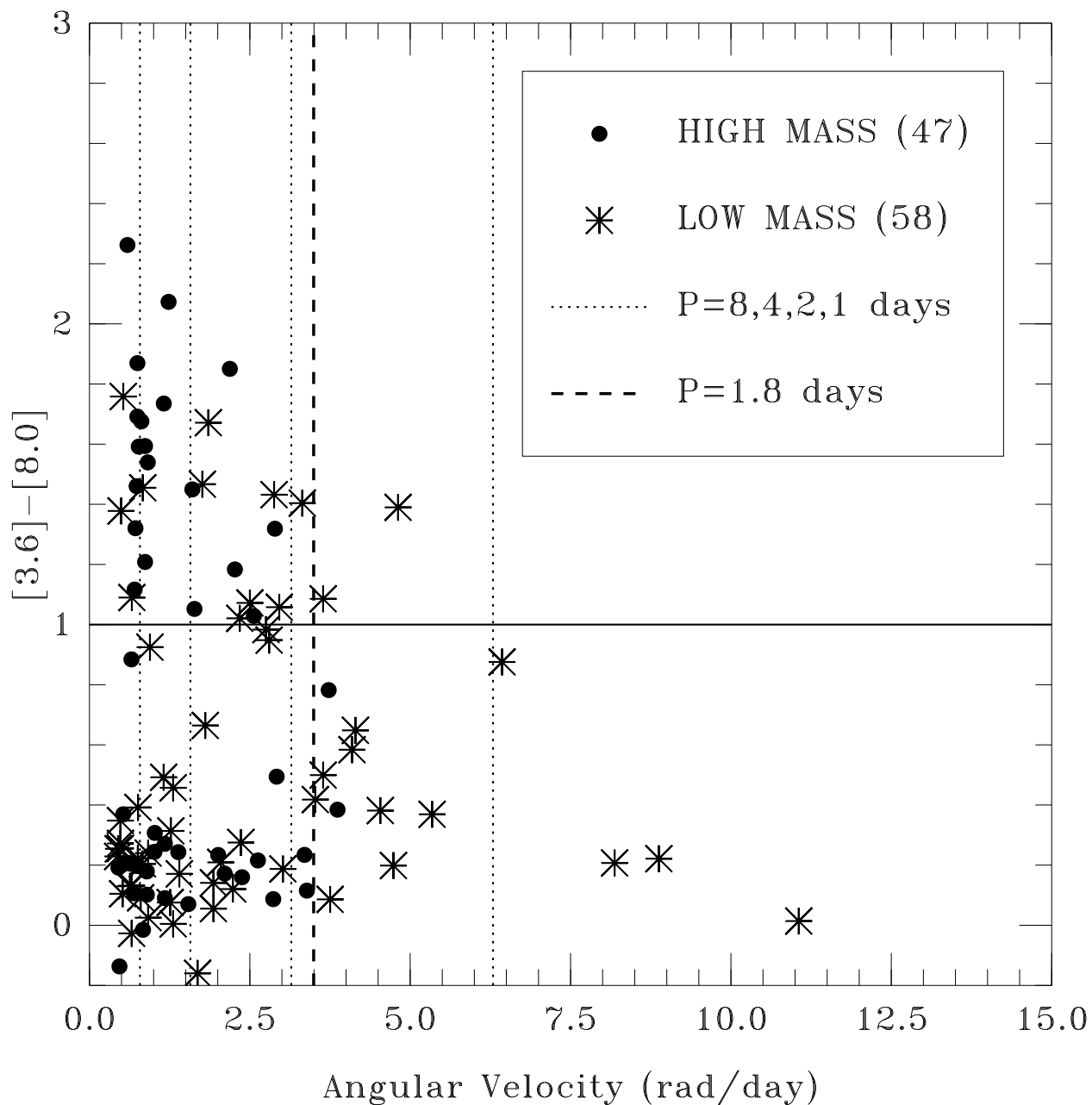


Fig. 11.—  $[3.6] - [8.0]$  color *vs.* angular velocity for low- and high-mass stars. Stars with periods  $\lesssim 1.5$  days are significantly less likely to have a disk than stars with longer periods. The low disk frequency of very fast rotators is the only feature of our sample that could *potentially* be interpreted as an evidence for disk braking, but a more rigorous analysis of this result is necessary to determine its significance.